Published for SISSA by Springer

Received: December 10, 2013
Accepted: January 25, 2014
Published: February 24, 2014

A holographic quantum Hall ferromagnet

C. Kristjansen,[a] **R. Pourhasan**[b,c] **and G.W. Semenoff**[d,e]

[a] *Niels Bohr Institute, Copenhagen University, Blegdamsvej 17, 2100 Copenhagen Ø, Denmark*
[b] *Perimeter Institute for Theoretical Physics, 31 Caroline St. N., Waterloo, ON, N2L 2Y5, Canada*
[c] *Department of Physics & Astronomy, University of Waterloo, Waterloo, Ontario N2L 3G1, Canada*
[d] *Department of Physics and Astronomy, University of British Columbia, Vancouver, BC V6T 1Z1, Canada*
[e] *International Institute of Physics, Federal University of Rio Grande do Norte, Av. Odilon Gomes de Lima 1722, Capim Macio, Natal-RN 59078-400 Brazil*

E-mail: kristjan@nbi.dk, rpourhasan@perimeterinstitute.ca, gordonws@phas.ubc.ca

Abstract: A detailed numerical study of a recent proposal for exotic states of the D3-probe D5 brane system with charge density and an external magnetic field is presented. The state has a large number of coincident D5 branes blowing up to a D7 brane in the presence of the worldvolume electric and magnetic fields which are necessary to construct the holographic state. Numerical solutions have shown that these states can compete with the the previously known chiral symmetry breaking and maximally symmetric phases of the D3-D5 system. Moreover, at integer filling fractions, they are incompressible with integer quantized Hall conductivities. In the dual superconformal defect field theory, these solutions correspond to states which break the chiral and global flavor symmetries spontaneously. The region of the temperature-density plane where the D7 brane has lower energy than the other known D5 brane solutions is identified. A hypothesis for the structure of states with filling fraction and Hall conductivity greater than one is made and tested by numerical computation. A parallel with the quantum Hall ferromagnetism or magnetic catalysis phenomenon which is observed in graphene is drawn. As well as demonstrating that the phenomenon can exist in a strongly coupled system, this work makes a number of predictions of symmetry breaking patterns and phase transitions for such systems.

Keywords: AdS-CFT Correspondence, Holography and condensed matter physics (AdS/CMT)

ArXiv ePrint: 1311.6999

doi:10.1007/JHEP02(2014)097

Contents

JHEP02(2014)097

1 Introduction and summary

The quantum Hall effect is one of the most dramatic phenomena in condensed matter physics [1, 2]. At particular values of its charge density and magnetic field, a two-dimensional electron gas exhibits incompressible charge-gapped states. These states can be robust and persist over a range of the ratio of density to field, that is, over a Hall plateau on which the Hall conductivity is a constant ν times the elementary unit of conductivity $\frac{e^2}{h}$ ($= \frac{1}{2\pi}$ in the natural units which we shall use in this paper),

$$\sigma_{xy} = \frac{\nu}{2\pi}. \tag{1.1}$$

The same electron gas can exhibit an array of such states, where ν is generally an integer, for the integer quantum Hall effect, or a rational number for the fractional quantum Hall effect.

What is more, the integer quantum Hall effect has a beautiful and simple explanation as a single-particle phenomenon. When a charged particle moving in two dimensions is exposed to a magnetic field, its spectrum is resolved into discrete Landau levels. Landau levels are flat, dispersionless bands with gaps between them. Fermi-Dirac statistics dictates that the low energy states of a many-electron system are obtained by filling the lowest energy single-electron states, with one electron per state. When a Landau level is completely filled with electrons, the next electron one inserts into the system must go to

the next higher level which is separated from the ones that are already occupied by a gap. The result is a jump in the chemical potential. Alternatively, when the chemical potential is in the gap between levels, it can be varied with no change of the charge density. Such a state is said to be incompressible. This effect is enhanced by disorder induced localization which forms a mobility gap and results in the Hall plateau.

In the absence of disorder, for free electrons, the Hall conductivity is given by (1.1) with ν equal to the filling fraction. The filling fraction is defined as the ratio of the number of electrons to the number of states in the Landau levels which are either completely or partially occupied (see (1.3) below). When a number of Landau levels are completely filled, ν is an integer which coincides with the number of filled levels and the Hall conductivity is quantized. It is given by the formula (1.1). Moreover, for completely filled energy bands, the Hall conductivity is a topological quantum number insensitive to smooth alterations of the energy band [3]–[5], such as those caused by changes in the environment of the single electrons. We can turn on lattice effects and disorder with the Hall conductivity remaining unchanged, and can thus conclude that, when ν is an integer, the quantized Hall conductivity is robust for a large range of single-particle interactions including the effects of disorder which are responsible for forming the Hall plateaus.

In addition to this, there are good theoretical arguments for the persistence of the integer Hall effect in the presence of electron-electron interactions, at least when the interactions are weak enough that perturbation theory can be applied. An easy way to understand this is by noting that, at the level of a low energy effective action, the Hall effect is encoded in a Chern-Simons term for the photon field,

$$S_{\rm CS} = \frac{\sigma_{xy}}{2} \int d^3x\, \epsilon^{\mu\nu\lambda} A_\mu \partial_\nu A_\lambda \ . \tag{1.2}$$

The coefficient of the Chern-Simons term is proportional to the Hall conductivity. Moreover, there is a theorem which states that the Chern-Simons term does not renormalize beyond one-loop order in either a relativistic or non-relativistic field theory [6–8]. The theorem depends on the existence of a charge gap in the spectrum. If the gap closes it is known that either scalar or fermion charged matter can renormalize the Chern-Simons term [7]. Thus, as far as perturbation theory is valid, the existence of the integer quantum Hall effect after interactions are turned on is intimately tied to the question of whether the incompressible nature of the state due to the energy gap between Landau levels survives in the interacting theory.

In this paper, we shall discuss the question as to whether any features of the integer Hall effect can persist when the coupling is strong, beyond the reach of perturbation theory. The development of AdS/CFT duality between certain gauge field theories and certain string theories has given us a tool for solving the strong coupling limit of some quantum systems. In a recent paper [9], two of the authors have found an example of a strongly coupled quantum field theory which, in a state with non-zero charge density and when subject to an external magnetic field, exhibits incompressible states with integer quantized Hall conductivity. It occurs in a non-Abelian gauge field theory that has a well-established string theory dual, the D3-D5 system [10]–[11]. The string theory is quantitatively tractable in its

JHEP02(2014)097

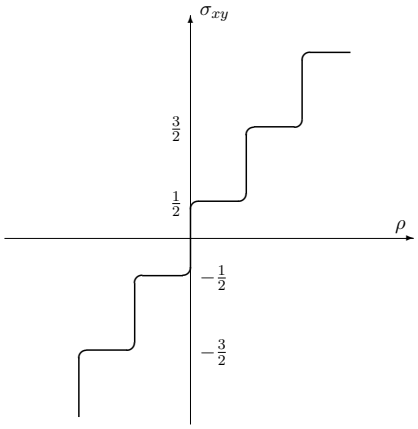

Figure 1. Integer quantum Hall effect in graphene. The vertical axis is the Hall conductivity in units of $4\frac{e^2}{h}$. The horizontal axis is the charge density at fixed magnetic field. The plateaus occur at the anomalous integer Hall conductivities $\sigma_{xy} = 4\,\frac{e^2}{h}(n + \frac{1}{2})$.

semi-classical low energy limit, and a further probe limit where the number of D5 branes is much smaller than the number of D3 branes. These limits coincide with the strong coupling and quenched planar limit of the quantum field theory and its solution yields information about the latter at strong coupling. The behavior of the theory when a charge density and magnetic field are added can readily be studied there. In that system, it was shown that there exist exotic states of the D3-D5 system where it becomes incompressible. These states occur at precisely integer values of the filling fraction ν, where

$$\nu \equiv \frac{2\pi\rho}{NB}, \tag{1.3}$$

with ρ the particle density, B the external field and N the number of colors of quarks in the non-Abelian gauge theory. These states were argued to be the natural strong coupling manifestation of some incompressible integer quantum Hall states which appear in the weak coupling limit of that theory.

Aside from a manifestation of an integer quantum Hall state, the incompressible states of the strongly coupled system found in reference [9] have an interesting analog in the observed quantum Hall states of graphene. Graphene is a two-dimensional semi-metal where the electron obeys an emergent massless Dirac equation with four flavors of the fermion field and an effective SU(4) symmetry [12, 13]. This fact leads to the anomalous quantum Hall effect [14, 15] where the Hall conductance is quantized as

$$\sigma_{xy}^{\text{graphene}} = \frac{e^2}{h} \cdot 4 \cdot \left(n + \frac{1}{2}\right). \tag{1.4}$$

The factor of 4 in this expression arises from the four-fold degeneracy of the low energy fermions and the offset of $1/2$ in $n + 1/2$ is a result of the spectrum of the massless Dirac fermions in a magnetic field. The Dirac Hamiltonian in a magnetic field has zero energy modes which form a Landau level at the apex of the Dirac cones. Particle-hole symmetry dictates that, in the ground state of the many-electron system, when it is charge neutral,

JHEP02(2014)097

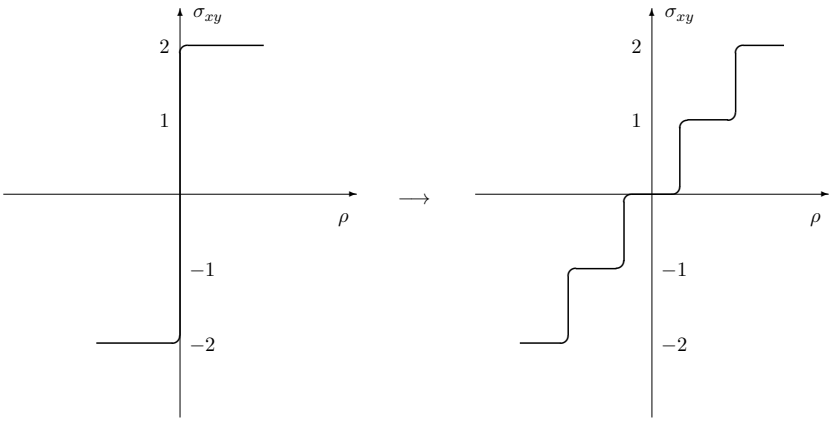

Figure 2. Quantum Hall Ferromagnetism/Magnetic Catalysis of chiral symmetry breaking in graphene. The four-fold degeneracy of all Landau levels is seen to be completely resolved in experiments with sufficiently clean samples with strong enough magnetic fields [18]. The vertical axis is the Hall conductivity in units of $\frac{e^2}{h}$. The horizontal axis is charge density at fixed magnetic field.

as well as all of the negative energy single electron states of the Dirac Hamiltonian, half of the zero modes should be filled . The neutral state is therefore not a Hall plateau. It has a half-filled Landau level and it is in the middle of a Hall step, as depicted in figure 1. These features were observed in the initial experiments which were performed soon after graphene was discovered in 2004 [16, 17].

Later, with stronger magnetic fields and cleaner samples, the formation of new plateaus were discovered at all of the integer steps. The four-fold degeneracy of the Landau levels is partially or completely lifted, depending on the filling fraction [18, 19]. The new plateaus are depicted in figure 2. In particular, the states which originate from the zero mode Landau level have interesting properties [20]–[22].

The mechanism for formation of these additional plateaus is thought to be spontaneous symmetry breaking and, like the integer Hall effect itself, it has a beautiful and elegant explanation at weak coupling. Here, we will focus on the charge neutral Landau level (near ρ=0 in figures 1 and 2). As we have already noted, in an external magnetic field, the single electron spectrum has zero modes and, when we construct the many-electron state in a certain range of densities, these single-electron zero modes must be partially filled. If electrons are non-interacting, a partially filled Landau level is a highly degenerate state, as any partial filling has the same energy as any other partial filling. In this circumstance, an interaction, no matter how weak, will generically split the degeneracy of these states. The most important electron-electron interaction in graphene is the Coulomb interaction. There are good arguments that suggest that, for the quarter-, half- or three-quarters filled zero mode Landau level, the Coulomb exchange interaction is minimized by states which resolve the four-fold degeneracy by spontaneously breaking the SU(4) symmetry. Once the symmetry is broken, energy gaps and Hall plateaus emerge at all integer filling fractions. This phenomenon is known in the condensed matter literature as quantum Hall ferromagnetism [23]–[30] and in the particle physics literature as magnetic catalysis of chi-

JHEP02(2014)097

ral symmetry breaking [31]–[44].[1] In experiments, this resolution is now seen for all of the integer Hall states [19] as well as the zero modes. In a clean system, the argument for symmetry breaking that we have reviewed here works at arbitrarily weak coupling and gives a candidate for an explanation of this interesting phenomenon.

However, graphene is not weakly coupled. The Coulomb interaction in graphene is putatively strong.[2] In fact, the magnitude of the energy gaps due to symmetry breaking that are seen in experiments is of order the Coulomb energy and they are already large enough to conclude that the system is strongly coupled. At a first pass, to understand the occurrence of this symmetry breaking in graphene, it is necessary to understand whether it can also happen in a strongly coupled system, that is, whether the features of quantum Hall ferromagnetism survive as the coupling constant is increased to large values. Reference [9] gives an affirmative answer to this question in the context of a certain quantum field theory. To be precise, the supersymmetric large N gauge field theory that is considered there cannot be regarded as a model of graphene in all of its details. On the other hand, as we shall outline below, it may be entirely possible that it does model some of the physics of the charge neutral Landau level in graphene. For this reason, among others, it is important to have an improved picture of the predictions of the model.

In this paper, we shall present a significant elaboration on the work in reference [9]. That work considered the D3-D5 system which is dual to a superconformal defect quantum field theory which has $\mathcal{N} = 4$ supersymmetric Yang-Mills theory living in the bulk of 3+1-dimensional spacetime. The 3+1-dimenisonal spacetime is bisected by an infinite, flat 2+1-dimensional defect. A 2+1-dimensional hypermultiplet field theory resides on the defect and interacts with the $\mathcal{N} = 4$ degrees of freedom in the 3+1-dimensional bulk. The defect field theory preserves half of the supersymmetry of the bulk $\mathcal{N} = 4$ theory and is conformally symmetric for all values of its coupling constant. The field theory living on the defect has both scalar and spinor fields and the Lagrangian is known explicitly [45, 46]. At weak coupling, its action contains massless fermions and bosons,

$$\mathcal{S} \sim \int d^3x \sum_{\alpha=1}^{N} \sum_{\gamma=1}^{N_5} \left[\bar{\psi}_a^{\alpha\gamma} i \partial\!\!\!/ \psi_{\alpha\gamma}^a - \partial_\mu \bar{\phi}_{\dot{a}}^{\alpha\gamma} \partial^\mu \phi_{\alpha\gamma}^{\dot{a}} \right] + \ldots , \tag{1.5}$$

which are fundamental representations of the gauged SU(N) color and the global U(N_5) flavor symmetries and are $(0, \frac{1}{2})$ and $(\frac{1}{2}, 0)$ representations of an SO(3)×SO(3) R-symmetry,

[1] These mechanisms usually focus on different order parameters and are sometimes thought to be mutually exclusive. In the present case, they are indistinguishable as a nonzero value of one order parameter will lead to a nonzero value of the other, and in fact the order parameters are equal in the weak coupling limit [38].

[2] The Coulomb energy of an electron-hole pair on neighboring sites is approximately 10 eV, whereas the tunnelling energy between the sites is about 2.7 eV. This is in line with the rough argument that the graphene fine structure constant which controls the quantum fluctuations of the photon is large: $\alpha_{\text{graphene}} = \frac{e^2}{4\pi\hbar v_F} = \frac{e^2}{4\pi\hbar c}\frac{c}{v_F} \approx \frac{300}{137}$ where we have used graphene's emergent speed of light which is a factor of 300 less than the speed of light in vacuum, $v_F \approx c/300$. This suggests that the Coulomb interaction in graphene is strongly coupled and out of the range of perturbation theory. Other indications such as the approximate perfect conical shape of Dirac cones seen in ARPES measurements [47] suggest that graphene dynamics is approximately scale invariant and has 2+1-dimensional Lorentz invariance over a significant range of energy scales. There is no known truly quantitative mechanism which would explain this.

JHEP02(2014)097

respectively. The masslessness of the fermions is protected by symmetry as there are no possible time reversal invariant mass operators which preserve all of the SU(N), U(N_5) and SO(3) $\times$ SO(3) symmetries. All solutions that we consider are invariant under color SU(N), the U(1) subgroup of U(N_5) and the first SO(3). We will consider solutions which break either the second SO(3) or the SU(N_5) subgroup of U(N_5) or both, and we will call this "chiral symmetry breaking" . This terminology will apply to any solution where the constant c_2 defined in equation (3.2) in section 3 is nonzero. This constant is called the "chiral condensate". The three dots in (1.5) indicate the action of $\mathcal{N} = 4$ Yang-Mills theory and interaction terms.

A constant U(1) $\subset$ U(N_5) external magnetic field, B, breaks supersymmetry. The free fermions and free bosons have different Landau level energies, $\omega_n = \pm\sqrt{2nB}$ and $E_n = \pm\sqrt{(2n+1)B}$, respectively, with $n = 0, 1, 2, \ldots$. The boson energies have a gap, $\sqrt{B}$. At energies lower than this gap, only the bosonic vacuum is relevant. On the other hand, the fermions have zero modes with degeneracy $2NN_5\frac{B}{2\pi}$. For states with filling fraction $\nu \leq N_5$ (with ν defined in equation (1.3)[3]), the lowest energy modes of the sufficiently weakly interacting theory are governed by the problem of populating the fermion zero modes. The arguments for quantum Hall ferromagnetism should apply to the $\mathcal{N} = 4$ gluon-mediated color interaction. In the large N planar limit in particular, the exchange interaction is emphasized and minimizing it should lead to breaking of the SO(3) chiral symmetry and, depending on the filling fraction, various symmetry breaking patterns for the U(N_5) flavor symmetry. The states with integer filling fractions $\nu = 0, \pm1, \pm2, \ldots, \pm N_5$ should be gapped, incompressible states with integer quantized Hall conductivities, though the series could truncate before it gets to $\pm N_5$ if the splitting of the states begins to compete with the energy of bosons, which begins at $\sqrt{B}$.[4] Also, the higher fermionic Landau levels are at energies greater than the threshold for creating bosons, so one would expect that they lead to no further incompressible states. We will see shortly that the counting of possible incompressible states is matched on the strong coupling side which is described by string theory.

The strongly coupled system is described by the embedding of N_5 coincident D5-branes in the $AdS_5 \times S^5$ background. At zero charge density and in the absence of magnetic fields, the D5-brane geometry is $AdS_4 \times S^2$, which has superconformal symmetry. The AdS_4 is a subspace of AdS_5. The S^2 is the maximal volume S^2 which can be embedded in S^5. The embedding position has an SO(3) symmetry so that an SO(3) $\times$ SO(3) subgroup of the SO(6) symmetry of S^5 survives.

Here, and everywhere in the following, we are considering boundary conditions for the embedding problem which do not violate the chiral symmetry of the gauge theory.

[3]Note that there is a factor of the number of colors, N, in the denominator of that equation. We are assuming that the SU(N) color symmetry remains unbroken. Thus, we take for candidate states only those which are singlets of the global color symmetry. For a many-body state of quarks to be a color singlet, the number of quarks must be an integer multiple of N. Therefore we consider states where the quarks come in multiples of N only. The filling fraction defined in (1.3) is the fractional occupancy of a Landau level where this natural N-fold degeneracy is taken into account.

[4]In addition, once supersymmetry and scale symmetry are broken by introduction of a magnetic field, there is no symmetry which prevents a boson mass term $m^2\bar{\phi}^{\alpha\gamma}_{\dot{a}}\phi^{\dot{a}}_{\alpha\gamma}$ from appearing in effective field theory. This would further isolate the fermion zero modes.

JHEP02(2014)097

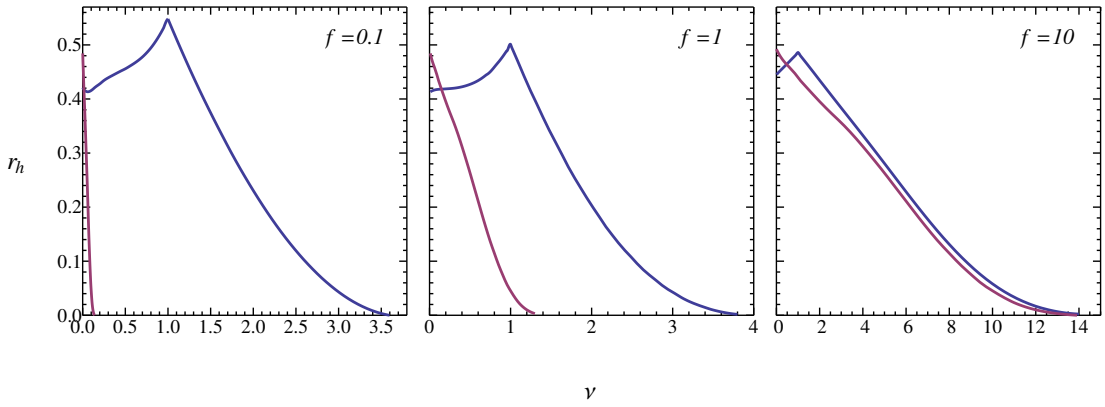

Figure 3. Chiral Symmetry Breaking: the wedge in the lower left below the red and blue lines are the regions where the Abelian D5 brane and the D7 brane, respectively, have lower energies than the chiral symmetric D5 brane. The horizontal axis is the filling fraction $\nu = \frac{2\pi\rho}{NB}$ and the vertical axis is the horizon radius (which is proportional to the temperature), in units of magnetic field. The parameter $f = \frac{2\pi N_5}{\sqrt{\lambda}}$ is proportional to the number of D5-branes. Plots for three different values of f are shown.

This means that, even for other solutions, the worldvolume geometry must approach this maximally symmetric $AdS_4 \times S^2$ geometry sufficiently rapidly as the D5 brane worldvolume approaches the boundary of $AdS_5 \times S^5$. In particular, the S^2 must become the SO(3)×SO(3) symmetric maximal S^2 and the N_5 multiple D5 branes must become coincident. The latter condition makes their boundary condition symmetric under SU(N_5). If the chiral symmetry is broken, it must be by spontaneous symmetry breaking. This symmetry breaking occurs if, as the D5 brane worldvolume stretches into the bulk of $AdS_5 \times S^5$, either the S^2 which the D5 brane wraps deviates at all from the maximal one of the most symmetric embedding, or the D5 branes spread apart, breaking the global SU(N_5) symmetry. We will encounter both of these behaviors shortly.

If we keep the charge density and the temperature at zero and introduce a constant external magnetic field, the D5 brane geometry changes drastically [37]. Near the boundary of $AdS_5 \times S^5$, the D5 brane is still $AdS_4 \times S^2$. However, as it enters the bulk of AdS_5, it pinches off and ends before it reaches the Poincare horizon of AdS_5, forming what is called a Minkowski embedding. It can pinch off smoothly without creating a boundary when a cycle shrinks to zero size. It is the S^2 which shrinks and chiral symmetry is spontaneously broken. Moreover, a Minkowski embedding has a charge gap due to the fact that charged excitations are open strings which must be suspended between the worldvolume and the Poincare horizon. When the worldvolume does not reach the Poincare horizon, these strings have a minimal length and therefore a gap in their energy spectrum. Thus, the strong coupling limit at $\nu = 0$ has an incompressible, charge-gapped state. This phenomenon is interpreted as the strong coupling manifestation of magnetic catalysis of chiral symmetry breaking. It is reasonable to conjecture that it is precisely the continuation to strong coupling of the formation of a gap at $\nu = 0$ in the neutral Landau level which we discussed at weak coupling. The symmetry breaking pattern is SO(3) × SU(N_5) → SO(2) × SU(N_5).

JHEP02(2014)097

When a charge density and a temperature are turned on, the chiral symmetry breaking phase survives for some range of these parameters, but it is eventually restored if the density or temperature become large enough.[5] The chiral symmetric phase of the D5 brane which is found at large enough temperature or density is simply one where the worldsheet is a product metric of the maximal S^2 embedded in S^5 and an asymptotically AdS_4 space, together with a configuration of worldvolume electro-magnetic fields which are needed to create the dual of the field theory with nonzero density and magnetic field.

The simple chiral symmetry breaking solutions of the D3-D5 system have been studied extensively in a number of contexts [48]–[56]. Their distinguishing feature can be characterized as "Abelian", in that the dynamics of each D5-brane in the stack of D5 branes is treated independently and their behaviors are all identical. The non-Abelian nature of the worldvolume theory does not play a role. The D5 branes remain coincident and have unbroken SU(N_5) symmetry. The phase diagram of these Abelian solutions is well known. It is reproduced in the numerical results of the present paper and corresponds to the red curves in figure 3, 4, and 8. More specifically, the lower-left-hand wedge in figure 3 is the region where the "Abelian" chiral symmetry breaking solutions of the D5-brane are stable. At the red line, the chiral symmetric competitor takes over, in the sense that it has lower energy. (The same red curve re-appears in figure 4 and figure 8.) A more detailed discussion with more details about this phase transition is given by Evans et al. [52].

The D7 brane is an alternative solution of the D5 brane theory.[6] It can be thought of as a "non-Abelian" configuration of D5 branes which is approximated by a D7 brane [9]. The stability region for the D7 brane in the temperature-density plane is similar to that of the Abelian D5 brane, but somewhat larger. It has less energy than the chiral symmetric competitor (the same competitor as for the Abelian D5 brane) to the lower left of the blue line in figure 3. The reader should beware that figure 3 does not compare the relative energies of the Abelian D5 and the D7 branes. This will be done in figure 4.

We now know of three competing solutions of the D3-D5 system, the Abelian D5 brane, the D7 brane and the chiral symmetric solution. (As we shall see later, for $\nu > 1$ we will in addition have the possibility of composite solutions.) To decide which is the preferred one at a given value of the temperature and filling fraction, we must compare their free energies. The free energy is a function of the temperature, the charge density, the magnetic field and the number of D5-branes, N_5. We will use a system of units where the magnetic field is equal to one. This leaves a normalized temperature, the filling fraction ν and the parameter

$$f \equiv \frac{2\pi N_5}{\sqrt{\lambda}}, \tag{1.6}$$

[5]The fact that the spontaneous breaking of a continuous symmetry in 2+1-dimensions survives at finite temperature would seem to contradict the Coleman-Mermin-Wagner theorem in the field theory. This is a typical artifact of the large N limit.

[6]An alternative solution of a D7 brane theory, called D7', has been studied extensively [57]–[62]. It also exhibits incompressible Hall states but with Hall conductivities that are given by irrational numbers. The main difference between that solution and the one that we study here is the behavior at the boundary of AdS_5. The D7 that we consider collapses to a D5 brane there, and should therefore be thought of as a solution of the D3-D5 system whereas D7' remains a D7 brane.

JHEP02(2014)097

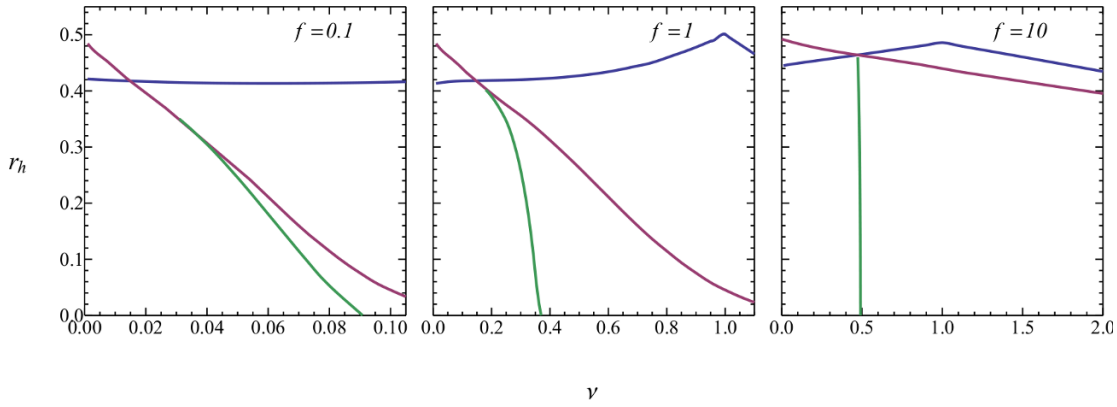

Figure 4. Phase diagram extracted from numerical data: the red and blue lines are taken from figure 3. These are lines where the chiral symmetric D5 brane has the same energy as the D5 brane (red) and the D7 brane (blue). The chiral symmetric phase is always more stable to the right and toward the top of the figure. The green line is where the Abelian D5 brane and the D7 brane have the same energy with the Abelian D5 preferred to the left and the D7 preferred to the right. The axes and values of f are as in figure 3.

as the variables which define the thermodynamic problem. We have done a numerical calculation of the energies of the three competing solutions. Before we begin to describe it, we warn the reader that, later on, we will find a completely different structure that takes over when the filling fraction ν is greater than or equal to one, and where the temperature is low. Thus, in the end, the following discussion will only apply to the region $0 < \nu < 1$. We will ignore this fact for now and will pursue the following discussion of the relative stabilities of the three solutions that we know about so far for all values of ν.

In figure 4, the regions where the Abelian D5 brane and the D7 brane are more stable than the chiral symmetric solution are displayed for three values of f. In all cases, the chiral symmetric solution is stable in the upper right-hand part of the diagram. The Abelian D5 brane is stable in the lower left, below the green line, that is, in all cases, for sufficiently small filling fraction and low temperature. As we increase temperature or filling fraction to the green line, there is a phase transition and, beyond the green line, the D7 brane becomes the energetically preferred solution. It remains so until we approach the blue line where the chiral symmetric phase becomes more stable and chiral symmetry is restored. This part of the blue line is beyond the edge of the figures in 4 but can be seen in figure 3. In summary, at low temperatures, as we increase the filling fraction from zero, generically there are three phases. First, at low density is the Abelian D5 brane. At some value of the density, there is a phase transition to the D7 brane. Then, at a larger density yet, there is a phase transition to the chiral symmetric state.

At low temperatures, the phase transition at the blue line in figures 3 and 4 is likely always of first order. At zero temperature, the chiral symmetric phase can be shown analytically to be meta-stable beyond a critical density, which is also known analytically [51]

$$\nu_{\text{crit}} \approx 1.68 f. \tag{1.7}$$

JHEP02(2014)097

In all of the cases where we have computed it, the blue line always occurs at higher values of ν.[7] This means that there is always a region where the D7 brane has lower energy than a meta-stable chiral symmetric phase. In this region, there must be an energy barrier between the phases. This indicates a first order phase transition. In the case of the Abelian solution at zero temperature, it is known that the transition to the chiral symmetric phase occurs precisely at $\nu_{\rm crit}$ and it is BKT like [51]. This is the intersection of the red line with the horizontal axis in figures 3 and 4. It is a beautiful and rare example of a non-mean-field phase transition for probe D branes. However, in all of the cases that we have studied, including those in figure 4, the green line occurs at values ν smaller than $\nu_{\rm crit}$ and the D7 brane is more stable than either the Abelian D5 or the chiral symmetric D5 in this region — there is no BKT-like transition in these cases.

The three phases that we have discussed so far have distinct symmetry breaking patterns. The Abelian D5 brane phase breaks the SO(3) symmetry to SO(2), but preserves the SU(N_5) flavor symmetry. The D7 brane phase breaks both the SO(3) symmetry and the SU(N_5) leaving only a subgroup of simultaneous transformations in SO(3) and an SO(3) subgroup of SU(N_5). Then the chiral symmetric phase retains both the SO(3) and the SU(N_5). This pattern of symmetry breaking is one of the predictions of the holographic model. However, as we have warned the reader, further developments that we shall outline below will cut this scenario off when the filling fraction reaches $\nu = 1$. It is only the behavior which occurs in the interval where $0 < \nu < 1$ which will turn out to be a prediction of what we have done so far.[8] As we can see by inspecting figures 3 and 4, the first transition from Abelian D5 to D7 typically occurs in this interval whereas the second, from D7 to chiral symmetric D5 does not.

The Abelian D5 brane has the feature that, once a non-zero charge density is turned on, it can no longer have a Minkowski embedding. This means that the theory no longer has a charge gap. Without a magnetic field, this would be natural. The analog at weak coupling is a finite density of fermions which create a Fermi surface. There are always low energy excitations of a Fermi surface. Such a system is not gapped, and this is also what is seen for the Abelian D5 brane. However, the Abelian D5 brane also remains ungapped in an external magnetic field, for any value of the magnetic field and any nonzero density. In other words, besides the $\nu = 0$ state, the Abelian D5 brane solutions contain no incompressible states at non-zero filling fractions, even in arbitrarily strong magnetic fields.

The D7 brane, on the other hand, can have incompressible states at special nonzero values of the charge density [9]. The D7 brane should properly be regarded as a non-Abelian configuration of D5-branes. It arises in the D5 brane theory when the transverse coordinates of the N_5 embedded D5 branes, which are $N_5 \times N_5$ matrices, form a fuzzy

[7] For very large values of f, we have observed that the red and blue lines come closer together and it is possible that, for sufficiently large f, they will coincide. In that case, there could be a large f region where the the BKT-like transition from either the abelian D5 or D7 brane to the chiral symmetric phase would still exist.

[8] Of course, in a real two dimensional electron gas, the physics of some of the region that we are talking about here is dominated by other effects such as impurities and localization. Our prediction could still apply to the symmetries of the Hall plateaus which are formed by these other effects. The other possibility is the clean limit which is thus far proven difficult to achieve, even in graphene.

JHEP02(2014)097

sphere.[9] It would be interesting to understand this "non-Abelian" configuration of the D5 brane better from this point of view. We shall not do this in the following. Instead, we simply approximate it by a classical D7 brane which wraps both of the S^2's in S^5. The second S^2 is the classical limit of the fuzzy sphere. The D7 brane remembers its origin as N_5 D5 branes by supporting a magnetic flux with Dirac monopole number N_5 on the second S^2. This approximation should be good when the number of D5 branes, N_5, is much greater than one, but still much less than N. In the asymptotic region near the boundary of $AdS_5 \times S^5$ the D7 brane has geometry $AdS_4 \times S^2 \times S^2$ where one S^2, the same one which is wrapped by the Abelian D5 brane, is nearly maximal and the other S^2 shrinks to zero size as the boundary is approached. This sphere has magnetic flux and when it shrinks to zero size it leaves a singular magnetic source. This can be regarded as a point where a D5 brane is attached to the D7 brane and it occurs precisely at the boundary of AdS_5.

In figures 3 and 4 there are peaks of the blue curves at $\nu = 1$. This is the special state of the D7 brane, where it has a Minkowski embedding and is incompressible with a charge gap. At low enough temperature, this state is energetically preferred over its competitors in the entire range of the parameter f that we have been able to study. Its existence also allows us to find an incompressible state for higher integer values of ν. This is gotten by simply taking ν D7 branes, each with filling fraction equal to one. As well as the charge density, which they share equally, the D7 branes must share the N_5 D5 branes between them. A numerical computation in reference [9] indicated that, at least for $\nu = 2$, first of all, the energy is minimized when the D5 branes are shared equally and secondly, the energy of two gapped $\nu = 1$ D7 branes with f shared equally between them is less than the energy of one ungapped $\nu = 2$ D7 brane or Abelian D5 brane. The second of these results tells us that the $\nu = 2$ gapped state with 2 D7 branes is preferred over the other possible ungapped states. The first one tells us that the gapped state is a state with two coincident gapped D7 branes. We conjecture but have not checked that this pattern persists to higher values of ν. Here, we shall assume that when the charge density is shared equally, the branes also prefer to share N_5 D5 branes equally. Indeed, this state has more symmetry than the alternatives, since the ν D7 branes are identical and coincident, and therefore have an unbroken internal gauge symmetry SU(ν). This would be an unbroken global symmetry

[9] S^5 is the locus of $n_1^2 + \ldots + n_6^2 = 1$ for real numbers $(n_1, \ldots, n_6)$. The two S^2's are loci of $n_1^2 + n_2^2 + n_3^2 = \sin^2\psi$ and $n_4^2 + n_5^2 + n_6^2 = \cos^2\psi$. All D5 and D7 brane solutions which we discuss wrap the first sphere, (n_1, n_2, n_3), and its SO(3) isometry is preserved. For the D5 brane, (n_1, n_2, n_3) are longitudinal coordinates and (n_4, n_5, n_6) are transverse coordinates. The chiral symmetric D5 brane sits at a higher symmetry point $n_4 = n_5 = n_6 = 0$ (or $\psi = \frac{\pi}{2}$) and preserves the second SO(3) symmetry. The Abelian D5 solution has some of the (n_4, n_5, n_6) non-zero. This breaks the second SO(3) (and preserves SU(N_5)). The D7 brane is a non-Abelian D5 brane where (n_4, n_5, n_6) are $N_5 \times N_5$ matrices in the SU(N_5) Lie algebra and which form an irreducible representation of an SO(3) subalgebra of SU(N_5),

$$[n_a, n_b] = i\epsilon_{abc} n_c \ . \tag{1.8}$$

The D7 brane preserves an SO(3) which is a combination of the SO(3) of the second S^2 and the SO(3) subgroup of SU(N_5). A time reversal invariant fermion mass operator (and order parameter for chiral symmetry breaking) which is invariant under the residual symmetry would be $m\bar{\psi} n_a \sigma^a \psi$. In the classical description as a D7 brane wrapping the second S^2 with N_5 units of monopole flux, the unbroken symmetry is the magnetic translation group on the S^2.

JHEP02(2014)097

of the field theory dual. Of course, in the strict sense, it can only happen if ν is an integer divisor of N_5. However, in the large N_5 limit that we are considering, the N_5 D5 branes can always be split equally to precision $\frac{1}{N_5}$ and the residual symmetry would be there to a very good approximation. This symmetry would be a subgroup $\mathrm{SU}(\nu) \subset \mathrm{SU}(N_5)$ which (in addition to some SO(3)'s), survives dynamical symmetry breaking by D7 branes. Its existence can be regarded as a prediction of our hypothesis for finding the charge gapped state with integer filling fraction ν.

Now, we are ready to take the next step and understand the ungapped states in the region between integer filling fractions, say the region $1 \leq \nu \leq 2$. At $\nu = 1$ the stable state is the gapped D7 brane. If we increase ν slightly, we might expect that the lowest energy state is a composite brane made from the same gapped D7 brane and either an ungapped Abelian D5 brane or an ungapped D7 brane where, in both cases, the second, ungapped brane takes on a share of the filling fraction, $\nu - 1$. In addition to this, the gapped and ungapped branes must share the N_5 D5 branes between them. Exactly how N_5 is distributed between the branes in the composite system is a dynamical question which we shall solve numerically in a few cases.[10]

Our investigation shows that, which ungapped brane is stable depends on the total N_5 through the parameter f defined in (1.6). If f is big enough, the Abelian D5 brane wins, and the state just above $\nu = 1$ is a hybrid of the gapped D7 brane and the ungapped Abelian D5 brane. Then, there is a phase transition in this intermediate region $\nu \in [1, 2]$, at a critical value of ν, to a state which is a composite of the gapped D7 and an ungapped D7 brane. As ν is increased further, and $\nu = 2$ approached from smaller values of ν, the state should be the gapped D7-ungapped D7 brane composite. When $\nu = 2$ is reached, as we have discussed above, it becomes two coincident gapped D7 branes, each with $\nu = 1$. At smaller values of f, our results indicate that the state just above $\nu = 1$ is immediately a composite of the gapped D7 brane and the ungapped D7 brane. The Abelian D5 brane does not appear at all in the interval $1 \leq \nu \leq 2$.

A similar pattern of composite branes is repeated in the intervals between larger integer values of ν. We have investigated this by numerical computation and have found that it is indeed the case. We have explicit numerical solutions up to the interval $8 \leq \nu \leq 9$. We currently have no evidence that the pattern stops. We also find that, even when f is large enough that the Abelian D5 brane phase exists just above the lower integer ν's, this is so only of the smaller values of ν. At higher integers, the Abelian D5 phase ceases to occur and integer ν D7 branes immediately become a composite of the gapped D7 branes and an ungapped D7 brane when ν is increased beyond the integer value.

In summary, in the defect quantum field theory that we are studying, when the mag-

[10] In the non-Abelian picture, the transverse matrix-valued coordinates of the gapped D7-ungapped D7 brane composite would have the n_a in equation (1.8) block-diagonal,

$$n_a = \begin{bmatrix} L_a^{(1)} & 0 \\ 0 & L_a^{(2)} \end{bmatrix}$$

where $L_a^{(1)}$ is a $n \times n$ and $L_a^{(2)}$ is an $(N_5 - n) \times (N_5 - n)$ irreducible representation of SO(3), respectively. For the gapped D7-ungapped Abelian D5 brane composite, $L_a^{(2)}$ is replaced by 0.

JHEP02(2014)097

netic field is turned on, for any value of the field strength, the chiral symmetry is broken in that there is always a chiral condensate. However, there is a charge gap only when ν is an integer, either positive or negative, and for values of ν with magnitude no bigger than N_5. The series could truncate before it gets to $\nu = \pm N_5$. We have not seen numerical evidence for this truncation, mainly due to the fact that our analysis considers very large N_5 and smaller values of ν. Between the integer values of ν, even though there is a nonzero chiral condensate, there is no charge gap.

The symmetry breaking patterns are then quite interesting. Let us begin with the case where f is small enough that the only composite branes are gapped D7-ungapped D7 branes. Let us begin at $\nu = 0$. There, at $\nu = 0$, as soon as the magnetic field is turned on, the SO(3) is spontaneously broken to an SO(2) subgroup. The full SU(N_5) symmetry is preserved there. As ν is increased, this symmetry breaking pattern persists up to a phase transition at a critical value of ν between zero and one, where there is a phase transition. At that phase transition, the system goes to a phase where the only symmetry which survives is in a diagonal subgroup of SO(3) and an SO(3) subgroup of SU(N_5). This symmetry breaking pattern then persists until we reach $\nu = 1$, where it is also the symmetry of the charge gapped state which appears at $\nu = 1$. Then, when we increase ν beyond one, the pattern changes again. The composite gapped D7-ungapped D7 brane that is stable there preserves two diagonal SO(3)'s, one for each D7 brane. These consist of SO(3) rotations combined with rotations in two commuting SO(3) subgroups of SU(N_5). When we reach $\nu = 2$, this symmetry is enhanced once again. The diagonal SO(3)'s become degenerate and they are transformed into each other by an additional SU(2) subgroup of SU(N_5). That is, at $\nu = 2$, out of the original SO(3) $\times$ SU(N_5), the symmetry which survives is $[\mathrm{SO}(3)]^2 \times \mathrm{SU}(2)$. When we increase ν to values just above two, the stable solution being a two gapped D7-one ungapped D7 composite, the symmetries that existed at filling fraction two are still there and, in addition, another new diagonal SO(3) emerges so that the total is $[\mathrm{SO}(3)]^2 \times \mathrm{SO}(3) \times \mathrm{SU}(2)$. The latter is the symmetry of the third, gapped D7 brane. When we reach $\nu = 3$, the third diagonal SO(3) becomes degenerate with the first two, so that $[\mathrm{SO}(3)]^2 \times \mathrm{SO}(3) \times \mathrm{SU}(2)$ becomes $[\mathrm{SO}(3)]^3 \times \mathrm{SU}(3)$. As far as we have investigated, this pattern repeats itself as we proceed to higher values of ν. At $\nu = n$, out of the original SO(3) $\times$ SU(N_5), the symmetry which survives is $[\mathrm{SO}(3)]^n \times \mathrm{SU}(n)$. When ν is just above n, this gets an additional SO(3) to become $[\mathrm{SO}(3)]^n \times \mathrm{SO}(3) \times \mathrm{SU}(n)$. When we reach $\nu = n + 1$ this is enhanced again to $[\mathrm{SO}(3)]^{n+1} \times \mathrm{SU}(n + 1)$. Of course, we know this reliably only when $n \ll N_5$. To study what happens for larger values of n is beyond our current ability, but would indeed be very interesting.

If the parameter f is larger, the additional composite phase, where there are n gapped D7 branes and an Abelian D5 brane, inserts itself in some of the regions just above $\nu = n$. We find that this is so, at least for big enough values of f and for small enough values of n. We have seen that, for $f = 10$, this happens for $\nu = 1, 2, 3$ and it ends at $\nu = 4$. Thereafter the states are always composites of D7 branes. This phase involving D5 branes breaks the SO(3) of the second S^2 to SO(2), and it leaves its share of the SU(N_5) symmetry intact. It therefore has residual symmetry $[\mathrm{SO}(2)]^n \times \mathrm{SU}(n) \times \mathrm{SU}(N_5 - N_5^0)$ where N_5^0 is the number of D5 branes that are absorbed by the n gapped D7 branes in the composite, leaving a stack

JHEP02(2014)097

of $N_5 - N_5^0$ D5-branes for the Abelian D5 brane part of the composite. Then, somewhere in the interval $\nu = [n, n+1]$ we expect a phase transition where the ungapped Abelian D5 brane blows up to an ungapped D7 brane, so that $[\mathrm{SO}(2)]^n \times \mathrm{SU}(n) \times \mathrm{SU}(N_5 - N_5^0) \to [\mathrm{SO}(3)]^n \times \mathrm{SO}(3) \times \mathrm{SU}(n)$. At some big enough value of n, the intermediate composites with Abelian D5 branes cease to exist and the pattern of the preceding paragraph takes over.

These symmetry breaking patterns can be considered a prediction of our holographic model and it is interesting to ask whether they are relevant to any realistic system. Aside from the supersymmetric system that is modelled directly, there is some hope that the model also captures some of the physics of any electronic system with degenerate Landau levels and a strong repulsive interaction. If interactions are ignored entirely, $2N_5$ degenerate Landau levels have an effective $\mathrm{SU}(2N_5)$ symmetry. In our model, the interactions on the other hand, have only a smaller symmetry, $\mathrm{SO}(3) \times \mathrm{SU}(N_5)$. (We are also ignoring the other, first SO(3), which transforms the first S^2 in the string theory and acts on the scalar fields in the weakly coupled field theory.) We are only able to analyze the situation where N_5 is large. We might wonder whether some aspect of the symmetry breaking pattern survives for small values of N_5. Then, the generic prediction is that the $\nu = 0$ state, that is the one where half of the states are filled, has distinctly different symmetry from all of the others.

The most realistic possibility is $N_5 = 2$ which could match the symmetries (spin times valley) of graphene or the a bilayer quantum Hall system where the SO(3) is spin symmetry and the SU(2) transforms the layer index. In both of these cases, the valley/layer symmetry is only approximate. In graphene, the long ranged Coulomb interaction is SU(4) symmetric and short ranged parts reduce this symmetry to $\mathrm{SO}(3) \times Z_2$, which is sometimes approximated by $\mathrm{SO}(3) \times \mathrm{SU}(2)$ where further, weaker interactions break the SU(2) [27].

We could ask how our symmetry breaking patterns would be seen in the weak coupling states where the charge neutral Landau level is fractionally filled. Let us go back to weak coupling for a moment. Denote the completely empty four-fold degenerate Landau level as $|0>$ and the electron creation operator as $\psi^\dagger_{Pab}$ where P denotes a state in some basis of the degenerate single-electron states of the Landau level and a, b, each taking values $\uparrow, \downarrow$ are valley/layer and spin indices. To get a translation invariant state, we must create an electron within each degenerate state of the Landau level, that is we must fill all of the states denoted by P. We begin by half-filling the Landau level to get the $\nu = 0$ state. That state has SO(3) symmetry broken to SO(2), but still has good SU(2) symmetry. This should be the symmetry pattern of the $\nu = 0$ plateau. The weak coupling state that does this is

$$\prod_P \psi^\dagger_{P\uparrow\uparrow} \psi^\dagger_{P\uparrow\downarrow} \, |0>$$

which is, for each state P in the Landau level, a valley triplet and spin singlet. It thus breaks the valley symmetry and preserves the spin symmetry. (The inverse is also possible, where the spin symmetry is broken and the valley symmetry survives. Here we are not distinguishing spin and valley symmetries.)

Then, consider the one-quarter and three-quarter filled states. For graphene, these are the $\nu = -1$ and $\nu = 1$ states, respectively. Quarter filling is achieved by creating an

JHEP02(2014)097

electron in one quarter of the zero mode states. A simple candidate for such a state is

$$\prod_P \psi^\dagger_{P\uparrow\uparrow} \; |0>$$

which is both spin and valley polarized.[11] This state breaks both the spin and valley symmetry. This is a different symmetry breaking pattern than we found for our holographic state with $\nu = 1$. We can make a many body state with a symmetry breaking pattern which matches the holographic state. It would be the state

$$\prod_P \frac{1}{\sqrt{2}} \epsilon^{ab} \psi^\dagger_{Pab} \; |0> = \prod_P \frac{1}{\sqrt{2}} (\psi^\dagger_{P\uparrow\downarrow} - \psi^\dagger_{P\downarrow\uparrow}) \; |0> \tag{1.9}$$

This state is neither spin nor valley polarized. It is a singlet under a simultaneous spin and valley rotation, and a triplet under a spin rotation and a simultaneous valley inverse rotation. Since, for the fermion zero mode Landau level that we are discussing, the wave-function of the zero modes in a specific valley also occupy only one of the graphene sublattices [7], the other valley occupying the other sublattice, a flip of the valley index corresponds to a translation which interchanges the sublattices. Since the state (1.9) is left unchanged by a simultaneous flip of valley and spin indices, this state is then an anti-ferromagnet.

There is a state at three-quarters filling that has similar symmetries,

$$\prod_P \frac{1}{\sqrt{8}} \epsilon^{fa} \psi^\dagger_{Pab} \epsilon^{bc} \psi^\dagger_{Pcd} \epsilon^{de} \psi^\dagger_{Pef} \; |0>$$

This state is also spin and valley unpolarized. The fact that the integer $\nu \neq 0$ states are that way is a generic feature of the holographic model. Here, we see that it suggests a particular state for both $\nu = -1$ and $\nu = 1$. It would be interesting to see if this suggestion is realized in graphene or multilayer Hall systems. Recent experimental results seem consistent with this picture [19].

The remainder of the paper discusses the details of the work that has been summarized in this introduction. In section 2 we discuss the mathematical problem of embedding D5 and D7 branes in $AdS_5 \times S^5$. In section 3, we discuss the boundary conditions and the asymptotic behavior of the solutions that we are looking for. In section 4 we discuss the details of both the technique and results of our numerical computations. In section 5 we conclude and we discuss directions for further work.

2 The geometric set-up

We shall study D5 and D7 probe branes at finite temperature and density. We will embed them in the asymptotically $AdS_5 \times S^5$ black hole background using coordinates where the

[11] If graphene, say, were fully SU(4) symmetric, the SU(4) could be used to rotate this state to any other choice, so if the dynamics were SU(4) invariant, this would be the most general state. However, if the interactions are not fully SU(4) invariant, but are symmetric under SO(3) × SU(2) instead, this state would break both the SO(3) and SU(2) symmetries. What is more, it is not the unique choice for a quarter filled state. The holographic states suggest the alternative (1.9).

JHEP02(2014)097

	t	x	y	z	r	ψ	θ	ϕ	$\tilde{\theta}$	$\tilde{\phi}$
$D3$	×	×	×	×						
$D5$	×	×	×		×		×	×		
$D7$	×	×	×		×		×	×	×	×

Table 1. D3, D5 and D7 world volume coordinates.

metric has the form

$$ds^2 = \sqrt{\lambda}\alpha' \Big[r^2(-h(r)dt^2 + dx^2 + dy^2 + dz^2) + \frac{dr^2}{h(r)r^2} + d\psi^2 + \sin^2\psi(d\theta^2 + \sin^2\theta d\phi^2) + \cos^2\psi(d\tilde{\theta}^2 + \sin^2\tilde{\theta} d\tilde{\phi}^2) \Big], \quad (2.1)$$

Here, the coordinates of S^5 are a fibration of the 5-sphere by two 2-spheres over the interval $\psi \in [0, \pi/2]$. Furthermore, (t, x, y, z, r) are coordinates of the Poincare patch of AdS_5 and

$$h(r) = 1 - \frac{r_h^4}{r^4},$$

with r_h the radius of the event horizon. The Hawking temperature is $T = r_h/\pi$. The Ramond-Ramond 4-form of the IIB supergravity background takes the form

$$C^{(4)} = \lambda\alpha'^2 \left[h(r) r^4 dt \wedge dx \wedge dy \wedge dz + \frac{c(\psi)}{2} d\cos\theta \wedge d\phi \wedge d\cos\tilde{\theta} \wedge d\tilde{\phi} \right], \quad (2.2)$$

Here, $\partial_\psi c(\psi) = 8\sin^2\psi\cos^2\psi$ and for later convenience we choose

$$c(\psi) = \psi - \frac{1}{4}\sin 4\psi - \frac{\pi}{2}. \quad (2.3)$$

The choice of integration constant is a string theory gauge choice and our results will not depend on it.

We will study D5 and D7 branes as well as some composite systems thereof in this background using the probe approximation where the number of probe branes N_5 and N_7 is much smaller than the number, N, of D3-branes. The world volume coordinates of our probe branes will be as given in the table above.

2.1 Probe D5 branes

Probe D5 branes are described by the DBI plus WZ actions, i.e.

$$S_5 = \frac{T_5}{g_s} N_5 \int d^6\sigma \left[-\sqrt{-\det(g + 2\pi\alpha'\mathcal{F}_5)} + 2\pi\alpha' C^{(4)} \wedge \mathcal{F}_5 \right], \quad (2.4)$$

where g_s is the closed string coupling constant, which is related to the $\mathcal{N} = 4$ Yang-Mills coupling by $4\pi g_s = g_{YM}^2$, σ^a are the coordinates of the D5 brane worldvolume, $g_{ab}(\sigma)$ is the induced metric of the D5 brane, $\mathcal{F}_5$ is the worldvolume gauge field and

$$T_5 = \frac{1}{(2\pi)^5 \alpha'^3}, \quad (2.5)$$

JHEP02(2014)097

is the D5 brane tension. The Wess-Zumino action will not contribute to the D5 brane equations of motion for the types of embeddings that we will discuss here. The overall factor of N_5 denotes the number of D5 branes. We are here assuming that the non-Abelian U(N_5) gauge symmetry structure of multiple N_5 branes plays no role. We shall take the world volume gauge field strength to be of the form

$$2\pi\alpha'\mathcal{F}_5 = \sqrt{\lambda}\alpha'\left[\frac{d}{dr}a(r)dr\wedge dt + bdx\wedge dy\right]. \tag{2.6}$$

Hence, we have a constant external magnetic field

$$B = \frac{\sqrt{\lambda}}{2\pi}\, b, \tag{2.7}$$

and a charge density ρ

$$\rho = \frac{1}{V_{2+1}}\frac{2\pi}{\sqrt{\lambda}}\frac{\delta S_5}{\delta \frac{d}{dr}a(r)}.$$

It is well known that there exists an embedding of the D5 brane with the world volume coordinates $(t, x, y, r, \theta, \phi)$ for which $\tilde{\theta}$, $\tilde{\phi}$ and z are constant and for which $\psi = \psi(r)$ depends only on r. For this embedding the world volume metric can be written as

$$\begin{aligned} ds^2 =& \sqrt{\lambda}\alpha'\Big[r^2(-h(r)dt^2 + dx^2 + dy^2) + \sin^2\psi(d\theta^2 + \sin^2\theta d\phi^2) \\ &+ \frac{dr^2}{h(r)r^2}\left(1 + h(r)\left(r\frac{d\psi}{dr}\right)^2\right)\Big], \end{aligned} \tag{2.8}$$

and the DBI action becomes

$$S_5 = -\mathcal{N}_5 N_5 \int_0^\infty dr\; 2\sin^2\psi\sqrt{b^2+r^4}\sqrt{1 + h(r)\left(r\frac{d\psi}{dr}\right)^2 - \left(\frac{da}{dr}\right)^2}, \tag{2.9}$$

where, using (2.5),

$$\mathcal{N}_5 = \frac{T_5}{g_s}(\sqrt{\lambda}\alpha')^3(2\pi)V_{2+1} = \frac{2\sqrt{\lambda}N}{(2\pi)^3}V_{2+1}. \tag{2.10}$$

The factor $(\sqrt{\lambda}\alpha')^3$ comes from the overall factor in the worldvolume metric in equation (2.8), the factor of (2π) is from the integral over the worldvolume two-sphere[12] and the integral over (x, y, t) produces the volume factor V_{2+1}. To finalize the description of the embedding of the D5-brane we should determine the functions $\psi(r)$ and $a(r)$ by varying the action above. In the process of variation one can use the boundary condition

$$\lim_{r\to\infty}\psi(r) = \frac{\pi}{2}, \tag{2.11}$$

[12]It is half of the volume of the 2-sphere. The other factor of 2 is still in the action in front of $\sin^2\psi$. This notation is designed to match with the D7 brane, which we shall study in the next section, and to coincide with notation in reference [9].

JHEP02(2014)097

which, as we shall see later, is compatible with the equation of motion for ψ. Since the variable $a(r)$ enters the Lagrangian only via its derivative, $a(r)$ is cyclic and can be eliminated in favor of an integration constant using its equations of motion. The corresponding integration constant is (up to another constant factor) equal to the charge density ρ, hence

$$\rho = \text{const.}$$

Eliminating $a(r)$ via a Legendre transform, following the steps of reference [9], gives us the Routhian,

$$\mathcal{R}_5 = -\frac{\mathcal{N}_5 N_5}{f}\left(\frac{2\pi B}{\sqrt{\lambda}}\right)^{\frac{3}{2}}\int_0^\infty dr\ \mathcal{L}_5, \tag{2.12}$$

where

$$\mathcal{L}_5 = \sqrt{4\sin^4\psi f^2(1+r^4)+(\pi\nu)^2}\sqrt{1+h(r)\left(r\frac{d\psi}{dr}\right)^2}. \tag{2.13}$$

Here r is a dimensionless variable, obtained by rescaling $r \to r\sqrt{b}$, the quantity f is related to the total number of D5 branes, i.e

$$f = \frac{2\pi}{\sqrt{\lambda}}N_5, \tag{2.14}$$

and finally ν is the filling fraction

$$\nu = \frac{2\pi}{N}\frac{\rho}{B}. \tag{2.15}$$

To determine $\psi(r)$ we should now finally extremize the Routhian keeping ν fixed. This leads to the following equation of motion for $\psi(r)$

$$\begin{aligned}&\frac{h\left(r\frac{d}{dr}\right)^2\psi}{1+h\left(r\frac{d}{dr}\psi\right)^2}+hr\frac{d}{dr}\psi\left[1+\frac{8r^4\sin^4\psi f^2}{4\sin^4\psi f^2(1+r^4)+(\pi\nu)^2}\right]\\&-2\frac{r_h^4}{r^4}r\frac{d}{dr}\psi\left[1+\frac{1}{1+h\left(r\frac{d}{dr}\psi\right)^2}\right]-\frac{8\sin^3\psi\cos\psi f^2(1+r^4)}{4\sin^4\psi f^2(1+r^4)+(\pi\nu)^2}=0.\end{aligned} \tag{2.16}$$

where, now r_h is in magnetic units, i.e. it has been rescaled $r_h \to r_h/b^{\frac{1}{2}}$ so that

$$r_h^2 = \pi^2 T^2\frac{\sqrt{\lambda}}{2\pi B}. \tag{2.17}$$

Note that the D5-brane solutions will depend only on the ratio $\frac{\nu}{f}$ and on the temperature T in magnetic units.

JHEP02(2014)097

2.2 Probe D7 branes

For probe D7 branes the DBI plus WZ action reads

$$S = \frac{T_7}{g_s}\int d^{\,8}\sigma\left[-\sqrt{-\det(g+2\pi\alpha'\mathcal{F}_7)}+\frac{(2\pi\alpha')^2}{2}C^{(4)}\wedge\mathcal{F}_7\wedge\mathcal{F}_7\right], \tag{2.18}$$

where

$$T_7 = \frac{1}{(2\pi)^7\alpha'^4}, \tag{2.19}$$

is the D7 brane tension. Notice that here we are considering a single D7 brane. The world volume gauge field strength we take to be of the form

$$2\pi\alpha'\mathcal{F}_7 = \sqrt{\lambda}\alpha'\left(\frac{d}{dr}a(r)dr\wedge dt + bdx\wedge dy + \frac{f}{2}d\cos\tilde{\theta}\wedge d\tilde{\phi}\right). \tag{2.20}$$

The flux parameter, f, is the parameter defined in equation (2.14). It corresponds to N_5 Dirac monopoles on $\tilde{S}^2$. The magnetic field and the charge density are again given by expressions (2.7) and (2.1). We will now be interested in the embedding of the D7-brane with world volume coordinates $(t, x, y, r, \theta, \phi, \tilde{\theta}, \tilde{\phi})$ and we know that there exists an embedding for which z is a constant and $\psi = \psi(r)$ is a function of ψ only. The corresponding D7 brane world volume metric reads

$$\begin{aligned} ds^2 =&\sqrt{\lambda}\alpha'\left[r^2(-h(r)dt^2+dx^2+dy^2)+\frac{dr^2}{h(r)r^2}\left(1+h(r)\left(r\frac{d\psi}{dr}\right)^2\right)\right.\\ &\left.+\sin^2\psi(d\theta^2+\sin^2\theta d\phi^2)+\cos^2\psi(d\tilde{\theta}^2+\sin^2\tilde{\theta}d\tilde{\phi}^2)\right], \end{aligned} \tag{2.21}$$

and the action becomes

$$\begin{aligned} S_7 =&-\mathcal{N}_7\int_0^\infty dr\left[2\sin^2\psi\sqrt{(f^2+4\cos^4\psi)(b^2+r^4)}\times\right.\\ &\left.\times\sqrt{1+h(r)\left(r\frac{d\psi}{dr}\right)^2-\left(\frac{da}{dr}\right)^2}+2\frac{da}{dr}bc(\psi)\right], \end{aligned} \tag{2.22}$$

where, using (2.19),

$$\mathcal{N}_7 = \frac{2\lambda N}{(2\pi)^4}V_{2+1}. \tag{2.23}$$

Again to finalize the embedding we have to determine the functions $\psi(r)$ and $a(r)$ by varying the action. We will use the same boundary condition as before, i.e. the one given in (2.11) which again will indeed be compatible with the equations of motion for $\psi(r)$. In this connection it is convenient that we have chosen $c(\psi)$ as in equation (2.3). Similarly to before $a(r)$ is a cyclic variable which can be eliminated using its equation of motion and the corresponding integration constant is again equal to the charge density up to a constant factor (different from the one of the D5 case). We will be interested in the situation where

JHEP02(2014)097

we fix the integration constants so that the charge density, ρ, is the same for D5 branes and D7 branes. After eliminating $a(r)$ via a Legendre transformation as before we find the following Routhian

$$\mathcal{R}_7 = -\mathcal{N}_7 \left(\frac{2\pi B}{\sqrt{\lambda}}\right)^{\frac{3}{2}} \int_0^\infty dr \mathcal{L}_7, \tag{2.24}$$

with

$$\mathcal{L}_7 = \sqrt{4\sin^4\psi(f^2+4\cos^4\psi)(1+r^4)+(\pi(\nu-1)+2\psi-\frac{1}{2}\sin 4\psi)^2}\ \times \\ \sqrt{1+h(r)\left(r\frac{d\psi}{dr}\right)^2}, \tag{2.25}$$

where we have rescaled r in the same way as before $r \to r\sqrt{b}$ and where ν is defined in equation (2.15). From the Routhian we derive the following equation of motion for $\psi(r)$

$$\begin{aligned} 0 =& \frac{h\left(r\frac{d}{dr}\right)^2\psi}{1+h\left(r\frac{d\psi}{dr}\right)^2} - 2\frac{r_h^4}{r^4} r\frac{d}{dr}\psi\left[1+\frac{1}{1+h\left(r\frac{d}{dr}\psi\right)^2}\right] \\ &+ hr\frac{d\psi}{dr}\left[1+\frac{8r^4\sin^4\psi(f^2+4\cos^4\psi)}{4\sin^4\psi(f^2+4\cos^4\psi)(1+r^4)+(\pi(\nu-1)+2\psi-\frac{1}{2}\sin 4\psi)^2}\right] \\ &- \frac{8\sin^3\psi\cos\psi f^2(1+r^4)+4\sin^3 2\psi\cos 2\psi r^4+4\sin^2 2\psi(\pi(\nu-1)+2\psi)}{4\sin^4\psi(f^2+4\cos^4\psi)(1+r^4)+(\pi(\nu-1)+2\psi-\frac{1}{2}\sin 4\psi)^2}. \end{aligned} \tag{2.26}$$

The main difference between the Routhian for the D5 and D7 branes is the term arising from the charge density, it is $(\pi\nu)^2$ for the D5 brane and $(\pi(\nu-1)+2\psi-\frac{1}{2}\sin 4\psi)^2$ for the D7 brane. This difference comes from the presence of Wess-Zumino terms in the action for the D7 brane.

3 Characteristics of solutions

3.1 Asymptotic behaviour as $r \to \infty$

Looking at the equations of motions for $\psi(r)$ for the $D5$ branes and the D7 branes respectively, i.e. eqs. (2.16) and (2.26), one can check that the asymptotic behaviour $\psi(r) \to \frac{\pi}{2}$ as $r \to \infty$, assumed in their derivation, is indeed compatible with these. Expanding $\psi(r) = \frac{\pi}{2} + \delta\psi$ for large r one furthermore finds the following differential equation both for D5 and D7

$$\left(r\frac{d}{dr}\right)^2\delta\psi + 3\left(r\frac{d}{dr}\right)\delta\psi + 2\delta\psi = 0. \tag{3.1}$$

This equation has the solution $\delta\psi(r) = \frac{c_1}{r} + \frac{c_2}{r^2}$ and hence for large r

$$\psi(r) = \frac{\pi}{2} + \frac{c_1}{r} + \frac{c_2}{r^2} + \dots. \tag{3.2}$$

JHEP02(2014)097

Since the full equations of motions for $\psi(r)$ are second order differential equations the two integration constants c_1 and c_2 completely characterize the solution. In the dual field theory language c_1 is a quantity proportional to the bare mass of the fundamental representation fields and c_2 is proportional to the chiral condensate. In the present paper we will always be dealing with the mass less case, i.e. $c_1 = 0$.

It is easy to see that the constant function $\psi(r) = \frac{\pi}{2}$ is a solution of the equations of motion for all $r \in [r_h, \infty]$ both for the D5 brane and the D7 brane case. For zero temperature, $r_h = 0$, one can show that there is a certain critical value of ν/f below which the constant solution is unstable, more precisely[13]

$$\left(\frac{\nu}{f}\right)_{crit} = \frac{2\sqrt{7}}{\pi} \approx 1.68, \quad \text{for} \quad r_h = 0. \tag{3.3}$$

For $(\nu/f) < (\nu/f)_{crit}$ the stable solution of the equations of motion should hence be an r-dependent solution. When $r_h > 0$ we expect that $(\nu/f)_{crit}$ becomes smaller. A solution with $c_1 = c_2 = 0$ must necessarily be the constant solution. A solution with $c_1 = 0$ and $c_2 \neq 0$ can be viewed as showing spontaneous breaking of chiral symmetry. The phase transition which occurs when $(\nu/f) = (\nu/f)_{crit}$ is thus interpreted as a chiral symmetry breaking/restoring phase transition. This phase transition was found for the D5 brane in reference [51] and was shown to exhibit Berezinsky-Kosterlitz-Thouless scaling. For the D7 case numerical investigations have shown that there are r-dependent solutions even in some part of the region where the constant solution is supposed to be stable and that these solutions are energetically favoured compared to the constant one [9].

Finally, let us highlight that the Routhians become identical for the D5 branes and the D7 brane as $r \to \infty$ due to the identity

$$\mathcal{N}_7 = \frac{\mathcal{N}_5 N_5}{f}. \tag{3.4}$$

3.2 Asymptotic behaviour as $r \to r_h$

Let us consider first the zero temperature case, $r_h = 0$. Looking at the equation of motion for $\psi(r)$ for the D5 brane we see that for $r = r_h = 0$, the equation of motion for $\psi(r)$ reduces to

$$\left.\frac{\partial_\psi V_5}{2V_5}\right|_{r=r_h=0} = 0, \tag{3.5}$$

where the "potential" V_5 is given by

$$V_5 = 4\sin^4\psi f^2(1+r^4) + (\pi\nu)^2. \tag{3.6}$$

The angle ψ must hence come to an extremum of the potential V_5, i.e. we need that

$$\partial_\psi V_5|_{r=r_h=0} = 16\sin^3\psi\cos\psi f^2 = 0. \tag{3.7}$$

[13] Note that even though the D7 brane equations of motion depend on ν and f separately, the prediction for the location of the phase transition depends only on their ratio.

JHEP02(2014)097

There are only two possible solutions, $\psi = 0$ and $\psi = \frac{\pi}{2}$. The solution $\psi = 0$ corresponds to a minimum of the potential and the solution $\psi = \frac{\pi}{2}$ to a maximum. A minimum is preferred since the second derivative of is positive there. When $r_h = 0$, if we assume that $\psi \to \psi_0$ as $r \to 0$, the linearized equation in the vicinity of $r = 0$ is

$$\left(r\frac{d}{dr}\right)^2 \delta\psi + r\frac{d}{dr}\delta\psi - \frac{\partial_\psi^2 V_5(\psi_0)}{2V_5(\psi_0)}\delta\psi = 0$$

and the solution has the form

$$\psi \sim \psi_0 + \alpha_+ r^{-\frac{1}{2}\left[1+\sqrt{1+\frac{2\partial_\psi^2 V}{V}}\right]} + \alpha_- r^{-\frac{1}{2}\left[1-\sqrt{1+\frac{2\partial_\psi^2 V}{V}}\right]} + \dots$$

If ψ_0 is at a maximum of the potential, so that $\frac{2\partial_\psi^2 V_5(\psi_0)}{V_5(\psi_0)} < 0$, both exponents are negative or complex. To have a sensible solution, both α_+ and α_- must be zero. This means that, if we begin integrating the nonlinear ordinary differential equation for $\psi(r)$ from $r = 0$, the solution will be the constant, and this can only make sense if $\psi_0 = \frac{\pi}{2}$, which is the solution that we already know about. Coincidentally, $\frac{\partial_\psi^2 V_5(\pi/2)}{V_5(\pi/2)} < 0$, so this is a consistent picture. On the other hand, if ψ_0 is a minimum of the potential, $\frac{\partial_\psi^2 V_5(\psi_0)}{4V_5(\psi_0)} > 0$, and one exponent, α_+ is negative whereas the other α_- is positive. To have a sensible solution, α_+ must be zero. If, again we integrate the differential equation for ψ up from $r = 0$, some fixed value of α_- will lead to an asymptotic form (3.2) of $\psi(r)$ where both c_1 and c_2 are nonzero. We would then have to adjust α_- so that $c_1 = 0$ to find the type of solutions that we are discussing. Then c_2 is completely fixed by the solution of the equation. There is the third possibility that the potential is flat, $\frac{\partial_\psi^2 V_5(\pi/2)}{V_5(\pi/2)} = 0$, which in fact happens at the other extremum, $\psi_0 = 0$. Then α_+ must again be set to zero. But the exponent multiplying α_- vanishes and it would seem that the linearized equation is solved by any constant fluctuation of ψ. In this case, one must appeal to nonlinear effects to see that the correct choice of minimum is still $\psi = 0$, although the flatness of the potential in the vicinity leads to a very slow evolution of ψ toward $\psi = 0$ as $r \to 0$. A similar argument to the above applied to the $r \to \infty$ regime shows that there exist two normalizable modes of the equation for fluctuations of the angle ψ only when ψ approaches a maximum of the potential, which is the large r limit of (3.6). The unique maximum is $\psi = \frac{\pi}{2}$ which is the asymptotic value that we are using.

For the D7 brane similar considerations apply but the relevant potential is different. More precisely,

$$V_7 = 4\sin^4\psi(f^2 + 4\cos^4\psi)(1 + r^4) + (\pi(\nu - 1) + 2\psi - \frac{1}{2}\sin 4\psi)^2, \tag{3.8}$$

for which

$$\partial_\psi V_7|_{r=r_h=0} = 8\sin^2\psi\cos\psi\left(2f^2\sin\psi + 4(\pi(\nu-1)+2\psi)\cos\psi\right). \tag{3.9}$$

We observe that as in the D5 brane case the derivative of the potential vanishes for $\psi = 0$ and $\psi = \frac{\pi}{2}$. However, in this case there is a third zero of the derivative which satisfies

$$\frac{f^2}{2}\tan\psi_0 + \pi(\nu - 1) + 2\psi_0 = 0. \tag{3.10}$$

JHEP02(2014)097

As long as $0 < \psi_0 < \frac{\pi}{2}$, $\partial_\psi^2 V(\psi_0) > 0$ and this point is the minimum of the potential. For $\nu < 1$ there is always a solution to (3.10) in the interval $[0, \frac{\pi}{2}]$ but for $\nu > 1$ there is never such a solution. In summary, for $\nu < 1$, ψ_0 is always the minimum. When $\nu > 1$, the minimum is at the extreme point of the interval, $\psi = 0$. Another way to see this is by looking at higher derivatives of the potential. We find

$$\partial_\psi^2 V_7(\psi)\big|_{\psi=0} = 0, \qquad \partial_\psi^3 V_7(\psi)\big|_{\psi=0} = \frac{32}{3}(\nu - 1)\pi. \tag{3.11}$$

The vanishing second derivative implies that $\psi = 0$ is an inflection point. Note that the sign of the third derivative is different if ν is greater or less than one. If $\nu > 1$, the potential is decreasing as ψ approaches zero and the endpoint of the interval is a global minimum for the function restricted to the range $[0, \frac{\pi}{2}]$. On the other hand, if $\nu < 1$ it is increasing as ψ approaches zero, and the endpoint is a local maximum, the only minimum being at $\psi = \psi_0$.

The above applies for when $\nu > 1$ or $\nu < 1$. However, for the D7 brane, $\nu = 1$ is a special place. For $\nu = 1$ the potential $V_7(\psi)$ vanishes for $\psi = 0$ and the last term in eq. (2.26) diverges. The equation can still be fulfilled if ψ becomes zero at some value of $r = r_0 > r_h$ and if $d\psi/dr$ simultaneously diverges at r_0. This type of embedding of the D7 brane is known as a Minkowski embedding, the D7 brane pinches off at AdS radius r_0 and does not reach the horizon. It is not possible to have a Minkowski embedding for the D7 brane for other values of ν. For the D5 brane a Minkowski embedding would only be possible for vanishing charge density, i.e. for $\nu = 0$, a case we shall not be interested in here.

For $r_h \neq 0$, the equation of motion evaluated at $r = r_h$ is

$$0 = -4r_h \frac{d}{dr}\psi + \frac{\partial_\psi V(\psi)}{2V(\psi)} \tag{3.12}$$

This no longer requires that ψ goes to an extremum of the potential, but it determines the derivative of ψ at the horizon once a value of ψ is specified there.

3.3 Composite systems

As explained above the parameters of our N_5 probe D5 branes and our single probe D7 brane are adjusted in a particular way in order to allow the interpretation of the probe D7 brane as a blown up version of the N_5 D5 branes. More precisely we fix the flux through the extra 2-sphere wrapped by the D7 brane to fulfill the relation (2.14) and we adjust the charge density and the magnetic field so that it is the same for the D5 branes and the D7 brane. Starting from N_5 D5 branes with a given charge density one can, however, imagine other scenarios than all of them blowing up to a single D7 brane.

For instance n_5 D5 branes could blow up to a D7 brane and the rest remain D5 branes. The resulting brane configuration in the interior of AdS_5 would then be a single D7 brane with flux $f = \frac{2\pi}{\sqrt{\lambda}} n_5$ and $(N_5 - n_5)$ D5 branes. The charge density would have to be shared between the D5 branes which would remain D5 branes and those which would blow up, resulting in, for instance for initial filling fraction ν, the D7 branes having filling fraction $\nu - \nu_0$ and the remaining $D5$ branes having filling fraction ν_0.

JHEP02(2014)097

Similarly, the N_5 D5 branes could blow up to a larger number of D7 branes with different charge densities. In the most general case, starting from N_5 D5 branes with filling fraction ν we could have $N_5 - n_5$ D5 branes remaining D5 branes with filling fraction ν_0 and n_5 D5 branes blowing up to n_7 D7 branes with flux values $\{f_i\}_{i=1}^{n_7}$, and filling fractions $\{\nu_i\}_{i=1}^{n_7}$ where the parameters would have to fulfill

$$\nu = \nu_0 + \sum_{i=1}^{n_7} \nu_i, \qquad n_5 = \frac{\sqrt{\lambda}}{2\pi} \sum_{i=1}^{n_7} f_i. \tag{3.13}$$

Notice in particular that this implies that the Routhian of the composite system (assuming the components to be non-interacting) becomes identical to the simple D5 brane Routhian as $r \to \infty$.

We shall not study this most general composite system but limit ourselves to the case where $\nu_i = 1$, for all i, except possibly for one, and $0 \leq \nu_0 < 1$. The reason for this is that the $\nu = 1$ gapped D7 brane has a special status, being particularly favoured energetically and according to our previous studies [9] having the interpretation of a first quantized Hall level. Composite systems will be investigated in detail in section 4.4.

4 Numerical investigations

We wish first in subsection 4.1–4.3 to consider a situation where a single D7 brane can be viewed as a blown up version of N_5 D5 branes. Accordingly, we chose the same value of the B-field, the charge density and hence the filling fraction ν for the two systems. Obviously, r_h is also chosen to be the same for the two systems. Furthermore, we choose the flux of the D7 brane on the second two-sphere, $\tilde{S}^2$, to be given as $f = \frac{2\pi}{\lambda} N_5$. Subsequently, in subsection 4.4 we turn to considering the types of composite systems mentioned above. I all cases we will restrict ourselves to the massless case, i.e. $c_1 = 0$, cf. section 3.1.

4.1 Characteristic solutions

To generate a non-constant solution for $\nu \neq 1$ we generate from the differential equation a Taylor series for ψ as a function of r for r in the vicinity of r_h assuming some value ψ_0 for $\psi(r_h)$. This series expansion is then used to generate the initial data needed for the integration procedure. We finally determine the value of ψ_0 by demanding that the solution has $c_1 = 0$.

To generate a non-constant solution for $\nu = 1$ we generate from the differential equation a Taylor series solution for $r(\psi)$ for small ψ assuming some value r_0 for $r(\psi = 0)$. Then we use the value of $r(\psi)$ and $r'(\psi)$ as generated by this Taylor series expansion as input to our integration procedure. Analogously to above we determine the value of r_0 by demanding that the solution has $c_1 = 0$. In figure 5 we have plotted some solutions for $\psi(r)$ for $f = 10$ and $r_h = 0.2$ and various values of ν.

4.2 The stability lines for D5 and D7

As explained in subsection 3.1 the constant solution $\psi = \frac{\pi}{2}$ solves the equation of motion both for D5 branes and D7 branes for all values of the parameters but this solution is

JHEP02(2014)097

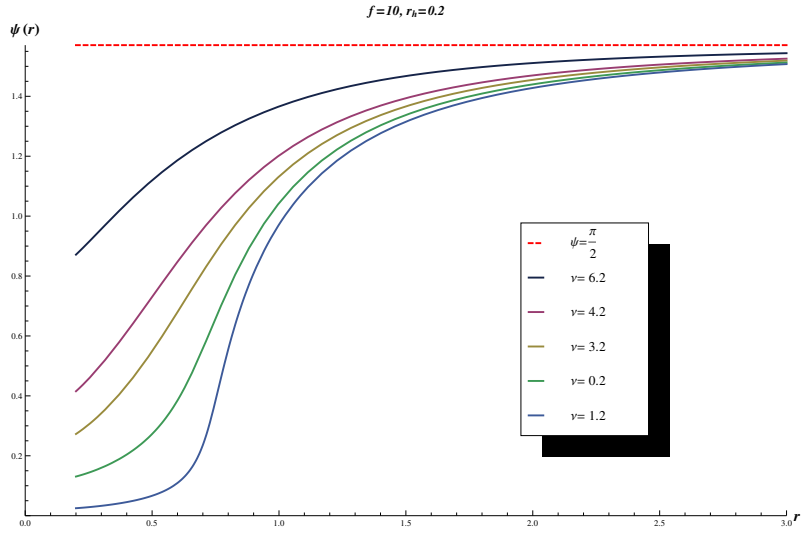

Figure 5. D7 brane solutions for $f = 10$ and $r_h = 0.2$ for various values of ν.

expected to be unstable when ν/f is small. For $r_h = 0$ the critical point below which the constant solution is unstable is given by $(\nu/f)_{crit} = \frac{2\sqrt{7}}{\pi}$. In this case, however, numerical studies show, that the non-constant D7 brane solution remains energetically favoured even in a part of the parameter space where the constant solution is stable [9].

One would expect that also for $r_h \neq 0$ one would have a region for small values of ν/f where the non-constant solution is energetically favoured. We have investigated this by comparing the energies of constant and non-constant solutions as determined from (minus) the corresponding values of the Routhian for various values of our parameters. Notice that whereas the total energy of any of the systems considered diverges (cf. eqs. (2.13) and (2.25)) energy differences between systems with identical values of the parameter f are finite.

In figure 3 we have shown the transition lines separating the region where the non-constant solution is energetically favoured from the region where the constant solution is the favoured one. The red curves correspond to D5 branes and the blue ones to D7 branes. Notice that non-constant D5 brane solutions depend only on ν/f whereas non-constant D7 brane solutions depend on ν and f separately. (The phase diagram for the D5 brane appeared already in [52].)

As for the zero-temperature case the D7 brane seems to have a much bigger region where the non-constant solution is favoured and very likely the non-constant solution again co-exists with the stable constant solution in a large part of the parameter space. The end point of the transition lines at $r_h = 0$ coincide with our previous zero-temperature estimates [9].

It is interesting to notice that the plots all have a peak corresponding to $\nu = 1$ which shows that this value of the filling fraction is particularly favoured. This is in agreement with our earlier interpretation of this state as the first quantum Hall level [9]. The special status of the $\nu = 1$ state implies that it is advantageous for the D branes to organize into composite systems for $\nu > 1$. We shall discuss this in detail in section 4.4.

JHEP02(2014)097

4.3 Crossover between D5 and D7 for $\nu < 1$

To the left of the blue curves in figure 3 the D5-branes and the corresponding D7 brane both have lower energy than the constant solution. It is thus interesting to investigate which one of these two has the lowest energy in the region $0 < \nu < 1$. (As already mentioned, when we pass the line $\nu = 1$, we in addition have composite systems to worry about and this case will be discussed in the following subsection.) We have earlier pointed out that the Routhians for the D5-branes and the D7 branes become identical when $r \to \infty$. We notice that for $r \to r_h$ the Routhians would coincide for $\nu = 1/2$ if for both systems the angle ψ would tend to zero at the horizon and a reasonable first guess for the location of the transition point could be at $\nu = 1/2$. (We know, however, that for the D7 brane when $r_h \neq 0$ and $\nu < 1$ the angle ψ does not tend to zero at the horizon, cf. section 3.2.)

In figure 4 we show in green the line of transition between D5 and D7 for $0 < \nu < 1$ for various values of f. The curve lies somewhat displaced from $\nu = \frac{1}{2}$ but approaches this line when f becomes larger.

4.4 Composite systems

As discussed above the gapped D7 brane with $\nu = 1$ is particularly energetically favoured. One can hence wonder whether composite systems could start playing a role when $\nu > 1$. Let us consider $\nu = 1 + \nu_0$, where $\nu_0 < 1$. For this value of ν one could imagine that n_5 of the N_5 D5 branes would blow up to a D7 brane with $\nu = 1$ and the rest either remain D5 branes with $\nu = \nu_0$ or blow up to another D7 brane with $\nu = \nu_0$. To see if this possibility is realized we have to compare the energy of the composite system with that of the simple D7 brane and D5 brane solution. The energy of the composite solution will of course depend on how many D5 branes blow up to gapped D7 branes and how many remain ungapped branes. The distribution of the D5 branes is reflected in the parameter f of the two components of the composite system. Let us denote the the flux of the gapped brane as f_0, i.e.

$$f_0 = \frac{2\pi}{\sqrt{\lambda}} n_5. \tag{4.1}$$

Then the f-parameter of the ungapped branes becomes $f_{\text{tot}} - f_0$ where f_{tot} is the f-parameter of the initial D5 branes. What we are interested in is the composite system for which the energy is the smallest possible one so for a given initial number N_5 of D5 branes and hence a given initial value of $f_{\text{tot}} = \frac{2\pi}{\sqrt{\lambda}} N_5$ we will have to find the value of f_0 which minimizes the energy of the composite systems. Naively one would expect that as many D5 branes as possible would blow up to gapped D7 branes but there are many dynamical issues which must be taken into account and we have to determine the minimum energy solution numerically.

In figure 6 we show an example for $f_{\text{tot}} = 1$ and $r_h = 0.2$ of how we sweep over different values of f_0 to determine the minimum possible energy for the composite system. Here we are considering a composite system consisting of a gapped D7 brane with $\nu = 1$ and a number of un-gapped D7 branes with $\nu = 0.3$. A similar sweep over values of f_0 must be done for the competing system consisting of gapped D7 branes supplemented with D5

JHEP02(2014)097

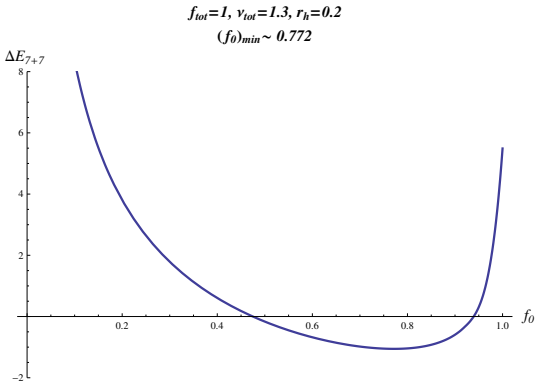

Figure 6. Plot for $f_{\rm tot} = 1$ and $r_h = 0.2$ showing the energy of a composite system consisting consisting of a gapped i.e. $\nu = 1$ D7 brane with flux f_0 and ungapped D7 branes with $\nu = 0.3$ and $f = 1 - f_0$ minus the energy of the constant solution with $\nu = 1.3$. The energetically favoured solution corresponds to $f_0 = 0.772$.

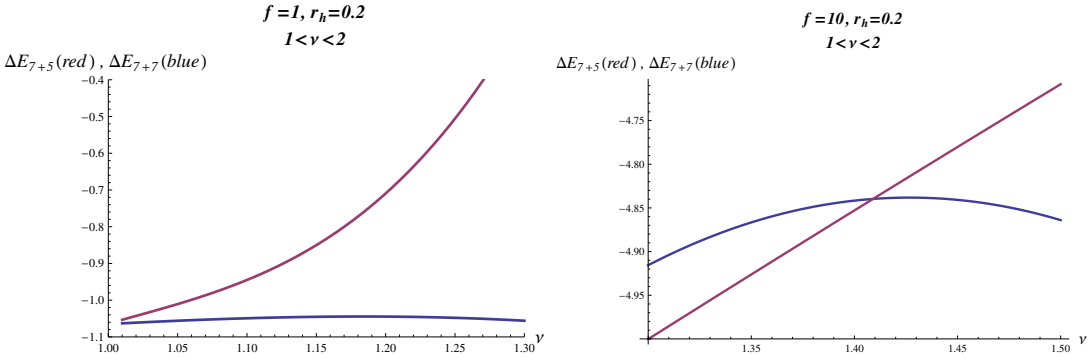

Figure 7. The difference between the energy of the composite D7-D5 system and the constant solution (red curves) and the difference between the energy of the composite D7-D7 system and the constant solution (blue curves) for $r_h = 0.2$ and $f = 1$ and $f = 10$ respectively. Notice the crossover at $\nu \approx 1.41$ for $f = 10$.

branes. Subsequently, we can compare the minimum energies of the the two composite systems and in addition we should compare these to the energy of the non-constant D7-brane solution with $\nu = 1.3$ and $f = 1$. (Had there been a non-constant D5 brane solution with similar parameters we would also have had to compare to the energy of this one but there is not.) In this way, i.e. by comparing energies, we are able to tell which system is the favoured one.

The case we have discussed pertains to the situation $1 < \nu < 2$. Let us now discuss what happens when we vary ν in this range. What we find is that when f is small the composite system consisting of gapped D7 branes plus un-gapped D7 branes is always the favoured one. However when f becomes larger, there appears at a certain value of ν a crossover between a region where the favoured composite system is D7 plus D5 and a region where the favoured composite system is D7 plus D7. In figure 7 we show for $r_h = 0.2$ and $f_{\rm tot} = 1$ the energy difference between the D7-D5 system and the constant solution (red curves) and the energy difference between the D7-D7 brane system and the

JHEP02(2014)097

constant solution (blue curves) for $f_{\rm tot} = 1$ and for $f_{\rm tot} = 10$ as a function of ν where $\nu \in [1, 2]$. Notice that to generate a given data point on each of these curves we first have to go through the minimization procedure described above and illustrated in figure 6. The curves tell us that for $f_{\rm tot} = 1$ and $r_h = 0.2$ the composite D7-D7 system is always the favoured one but for $f_{\rm tot} = 10$ and $r_h = 0.2$ there is a crossover between D5-D7 and D7-D7 at $\nu \approx 1.41$. We have repeated the analysis for different values of r_h and found that the crossover point does not show strong dependence on r_h.

Now we can move on to considering the interval $2 < \nu < 3$, i.e. a ν on the form $\nu = 2 + \nu_0$ where $0 < \nu_0 < 1$. In this interval we can have composite systems consisting of two gapped D7 branes with $\nu = 1$ in combination with either ungapped D7 branes or D5 branes. Again we have to determine by numerical investigations how many D5 branes blow up to gapped D7 branes and how many do not. In addition, we now in principle have the option that the two gapped D7 branes can have different values for the flux. However, we know from our previous analysis of the zero temperature case [9] that for a collection of gapped D7 branes with total flux f the energetically favoured situation is the one where the flux is equally shared between the D7 branes. If we denote the flux for each of the gapped D7 branes as f_0 the f-parameter for the un-gapped branes now becomes $f_{\rm tot} - 2f_0$. Again we have to sweep over f_0 to determine how precisely the branes of the composite systems organize themselves into gapped branes and ungapped ones. After having found the most favourable configuration for each of the two types of composite systems we can again compare their energies to each other and to the energy of the constant solution with $\nu = 2 + \nu_0$. What we find is that the pattern seen in the interval $1 < \nu < 2$ repeats itself. For small values of f the composite D7-D7 system always wins but when f becomes larger there starts to appear a cross over between D7-D5 and D7-D7. Again the cross over point does not depend very much on r_h.

It is obvious that we can now repeat the whole procedure again in the interval $3 < \nu < 4$ and in all the following intervals of the type $n < \nu < n + 1$ where we could have composite systems with n gapped D7 branes in combination with an ungapped D7 brane or with D5 branes. We have done the analysis for $r_h = 0.2$ and for intervals up to and including $\nu \in [8, 9]$. We have found that up to and including $\nu \in [4, 5]$ there is in each interval a transition between a region where the D7-D5 system is the energetically favoured one and another region where the D7-D7 system is favoured. The region where the D7-D5 system is favoured diminishes as ν increases and for $\nu > 5$ the D7-D7 system always wins. In figure 8 we show the full phase diagram for $f = 10$. The red and the blue curves are the stability lines for the D5 and the D7 branes from figure 3 and the vertical green lines are the lines which separate the composite D5-D7 systems from the composite D7-D7 systems.

5 Conclusion

The results of our numerical investigations and the conclusions that can be drawn from there are reviewed in the first section of this paper. In this concluding section, we wish to point out some interesting directions for further work on this subject, including some speculations about possible new results.

JHEP02(2014)097

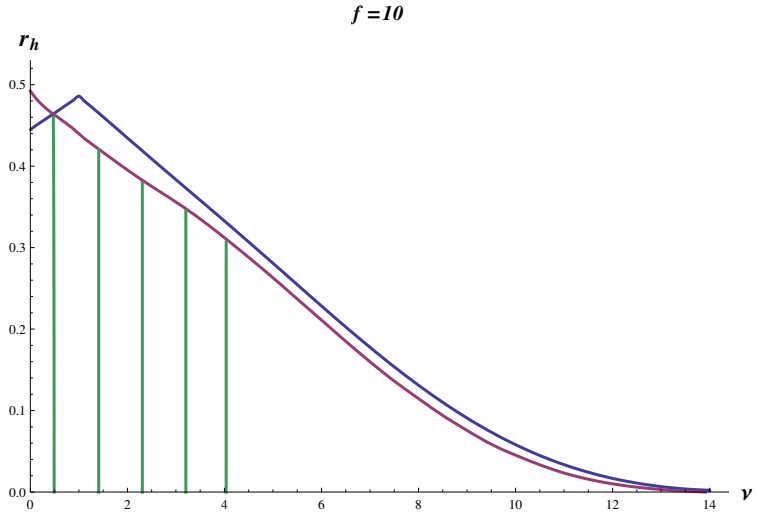

Figure 8. Plot for $f = 10$ showing a transition line (green) in each interval $[\nu, \nu + 1]$ with $\nu \in \{0, 1, 2, 3, 4\}$ separating the composite D5-D7 system with ν gapped D7 branes from the composite D7-D7 system, likewise with ν gapped D7 branes. For $\nu > 5$, the D7-D7 system always wins.

We have not explored the blown up solutions of the D5 brane from the D5 brane point of view where it would be a non-Abelian configuration of D5 branes. There are a number of obstacles to this approach, one being that the full generalization of the Born-Infeld action is not known when the embedding coordinates of the D brane are matrices. It would nevertheless be interesting to ask whether some of the features of the solution that we find are visible in the non-Abelian D5 brane theory. We expect that the approximation of the non-Abelian D5 brane as a classical D7 brane is good in the limit where the number of D5 branes is large. However, we also expect that the blow up phenomenon at $\nu = 1$ should also be there for a small number of branes and the only way to see it is from the non-Abelian D5 brane point of view.

We have done extensive numerical solutions of the embedding equations for the D5 and D7 branes. We have not analyzed the small fluctuations about these solutions. The spectrum of fluctuations would tell us, for example, if the solutions that we have found are stable or metastable. A search for further instabilities would be very interesting, especially considering that other D7 brane configurations are known to have instabilities to forming spatially periodic structures when the density is large enough.

Most excitingly, we have an observation about a possibly interesting electronic property of the ungapped D7 brane solutions. If we compare the numerical solutions of the ungapped Abelian D5 brane and the ungapped D7 brane, in the regions of the phase diagram where the D7 brane is favored, it has lower energy because it has an exceedingly narrow funnel. The funnel is the lower AdS radius part of the D brane world volume which is in the region where the brane approaches the Poincare horizon. Numerical computation in reference [9] already found this narrow funnel and we have confirmed it here. As we have discussed in section 1, when the filling fraction is not an integer, it is necessary for the D brane worldvolume to reach the Poincare horizon. This is due to the fact that the worldvolume

JHEP02(2014)097

electric fields that are needed to create the nonzero charge density state in the holographic theory need to end at a source, or else thread through the entire space. In a rough sense, the D brane creates the source in that it becomes narrow to emulate a group of suspended strings. In the case of the D7 brane, this funnel region is exceedingly narrow. In the dual field theory, this narrowness of the D brane funnel implies a very small density of electronic states at low energies. We liken this to the situation at weak coupling where localization due to impurities depletes the extended states, leading to a mobility gap. For the D7 brane, there is no mobility gap in the mathematical sense, but the density of conducting states is anomalously small. This scarcity of conducting states could lead to an approximate, dynamically generated quantum Hall plateau, a tantalizing possibility since the only other known mechanism for Hall plateaus is localization. This would give a strong coupling mechanism.

We have not found solutions of probe D5-brane theory which would be the holographic dual of fractional quantum Hall states. Such states are both predicted by theoretical arguments [64]–[69] and found experimentally [70]–[72] in graphene and they are normally taken as evidence of strong electron-electron correlations. The strong coupling limit that we can analyze using holography should be expected to see such states. One might speculate that solutions corresponding to fractional Hall states could be obtained from the integer quantum Hall states that we have already found by SL(2,Z) duality which has a natural realization in three dimensional Abelian gauge theory [73] and also a natural action on quantum Hall states [74, 75]. In particular, it can map integer quantum Hall states to fractional quantum Hall states. Exactly how this would work in the context of the present paper certainly merits further careful study. In particular, it could elucidate the relationship of the current work with other known string theory and holographic constructions of fractional quantum Hall states [76]–[79].

A beautiful aspect of the fractional Hall states found in reference [78] is the explicit construction of boundaries and the existence of boundary currents. In our construction, the Hall state has a charge gap and it must therefore be a bulk insulator. The Hall current should be carried by edge states. The edges must be at the asymptotic spatial boundaries. It would be interesting, following reference [78] to attempt to construct boundaries or domain walls which would carry the currents.

Another place that SL(2,Z) duality and alternative quantization have been exploited recently is in the holographic construction of an anyonic superfluid [80]. That construction was based on the D7' model which has non-integer quantized Hall states. It exploited the idea that, when the external magnetic field is made dynamical, so that it adjusts its own vacuum expectation value to the desired filling fraction, what was a quantum Hall state obtains a soft mode and becomes a compressible superfluid. It should be possible to apply similar reasoning to the construction that we have outlined in this paper. In this case, it would describe anyons based on integer level Chern-Simons theory.

Acknowledgments

C. Kristjansen was supported by FNU through grant number DFF-1323-00082. R. Pourhasan and G. Semenoff were supported by NSERC of Canada. R. Pourhasan was

JHEP02(2014)097

supported in part by Perimeter Institute for Theoretical Physics. Research at Perimeter Institute is supported by the Government of Canada through Industry Canada and by the Province of Ontario through the Ministry of Research and Innovation. R. Pourhasan would like to thank Niels Bohr Institute for their hospitality during the visit where part of this work was done. G. Semenoff acknowledges the kind hospitality and financial support of the International Institute of Physics in Natal, Brazil, where this work was completed.

JHEP02(2014)097

References

[1] T. Ando, A. B. Fowler and F. Stern, *Electronic properties of two-dimensional systems*, *Rev. Mod. Phys.* **54** (1982) 437.

[2] Z.F. Ezawa, *Quantum Hall effects: field theoretical approach and related topics*, World Scientific, Singapore (2000).

[3] R.B. Laughlin, *Quantized Hall conductivity in two-dimensions*, *Phys. Rev.* **B 23** (1981) 5632 [INSPIRE].

[4] D. Thouless, M. Kohmoto, M. Nightingale and M. den Nijs, *Quantized Hall conductance in a two-dimensional periodic potential*, *Phys. Rev. Lett.* **49** (1982) 405 [INSPIRE].

[5] Q. Niu, D.J. Thouless and Y.-S. Wu, *Hall conductance as a topological invariant*, *Phys. Rev.* **B 31** (1985) 3372.

[6] S.R. Coleman and B.R. Hill, *No more corrections to the topological mass term in QED in three-dimensions*, *Phys. Lett.* **B 159** (1985) 184 [INSPIRE].

[7] G.W. Semenoff, P. Sodano and Y.-S. Wu, *Renormalization of the statistics parameter in three-dimensional electrodynamics*, *Phys. Rev. Lett.* **62** (1989) 715 [INSPIRE].

[8] J.D. Lykken, J. Sonnenschein and N. Weiss, *The theory of anyonic superconductivity: a review*, *Int. J. Mod. Phys.* **A 6** (1991) 5155 [INSPIRE].

[9] C. Kristjansen and G.W. Semenoff, *Giant D5 brane holographic Hall state*, *JHEP* **06** (2013) 048 [arXiv:1212.5609] [INSPIRE].

[10] A. Karch and L. Randall, *Open and closed string interpretation of SUSY CFT's on branes with boundaries*, *JHEP* **06** (2001) 063 [hep-th/0105132] [INSPIRE].

[11] A. Karch and L. Randall, *Locally localized gravity*, *JHEP* **05** (2001) 008 [hep-th/0011156] [INSPIRE].

[12] G.W. Semenoff, *Condensed matter simulation of a three-dimensional anomaly*, *Phys. Rev. Lett.* **53** (1984) 2449 [INSPIRE].

[13] A.K. Geim and K.S. Novoselov, *The rise of graphene*, *Nat. Mater.* **6** (2007) 183.

[14] V. Gusynin and S. Sharapov, *Unconventional integer quantum Hall effect in graphene*, *Phys. Rev. Lett.* **95** (2005) 146801 [cond-mat/0506575] [INSPIRE].

[15] V. Gusynin and S. Sharapov, *Unconventional integer quantum Hall effect in graphene*, *Phys. Rev. Lett.* **95** (2005) 146801 [cond-mat/0506575] [INSPIRE].

[16] Y. Zhang, Y.-W. Tan, H.L. Stormer and P. Kim, *Experimental observation of the quantum Hall effect and and Berry's phase in graphene*, *Nature* **438** (2005) 201 [INSPIRE].

[17] K. Novoselov et al., *Two-dimensional gas of massless Dirac fermions in graphene*, *Nature* **438** (2005) 197 [cond-mat/0509330] [INSPIRE].

[18] Y. Zhang et al., *Landau-level splitting in graphene in high magnetic fields*, *Phys. Rev. Lett.* **96** (2006) 136806.

[19] A.F. Young et al., *Spin and valley quantum Hall ferromagnetism in graphene*, *Nature Phys.* **8** (2012) 553.

[20] D. A. Abanin et al., *Dissipative quantum Hall effect in graphene near the Dirac point*, *Phys. Rev. Lett.* **98** (2007) 196806 [cond-mat/0702125] [INSPIRE].

[21] J.G. Checkelsky, L. Li and N.P. Ong, *The zero-energy state in graphene in a high magnetic field*, *Phys. Rev. Lett.* **100** (2008) 206801.

[22] J.G. Checkelsky, L. Li and N.P. Ong, *Divergent resistance at the Dirac point in graphene: evidence for a transition in a high magnetic field*, *Phys. Rev.* **B 79** (2009) 115434 [arXiv:0808.0906] [INSPIRE].

[23] H.A. Fertig, *Energy spectrum of a layered system in a strong magnetic field*, *Phys. Rev.* **B 40** (1989) 1087.

[24] T. Jungwirth and A.H. MacDonald, *Pseudospin anisotropy classification of quantum Hall ferromagnets*, *Phys. Rev.* **B 63** (2000) 035305 [cond-mat/0003430] [INSPIRE]

[25] Z. Ezawa and K. Hasebe, *Interlayer exchange interactions,* SU(4) *soft waves and skyrmions in bilayer quantum Hall ferromagnets*, *Phys. Rev.* **B 65** (2002) 075311 [cond-mat/0104448] [INSPIRE].

[26] S.Q. Murphy et al., *Many-body integer quantum Hall effect: evidence for new phase transitions*, *Phys. Rev. Lett.* **72** (1994) 728.

[27] K. Moon et al., *Spontaneous interlayer coherence in double-layer quantum Hall systems: charged vortices and Kosterlitz-Thouless phase transitions*, *Phys. Rev.* **B 51** (1995) 5143 [cond-mat/9407031] [INSPIRE].

[28] K. Nomura and A.H. MacDonald, *Quantum Hall ferromagnetism in graphene*, *Phys. Rev. Lett.* **96** (2006) 256602.

[29] M.O. Goerbig, *Electronic properties of graphene in a strong magnetic field*, *Rev. Mod. Phys.* **83** (2011) 1193 [arXiv:1004.3396] [INSPIRE].

[30] Y. Barlas, K. Yang and A. Macdonald, *Quantum Hall effects in graphene-based two-dimensional electron systems*, *Nanotechnology* **12** (2012) 052001 [arXiv:1110.1069] [INSPIRE].

[31] K. Klimenko, *Three-dimensional Gross-Neveu model in an external magnetic field*, *Theor. Math. Phys.* **89** (1992) 1161 [INSPIRE].

[32] V. Gusynin, V. Miransky and I. Shovkovy, *Catalysis of dynamical flavor symmetry breaking by a magnetic field in* $(2+1)$*-dimensions*, *Phys. Rev. Lett.* **73** (1994) 3499 [*Erratum ibid.* **76** (1996) 1005] [hep-ph/9405262] [INSPIRE].

[33] V. Gusynin, V. Miransky and I. Shovkovy, *Dynamical flavor symmetry breaking by a magnetic field in* $(2+1)$*-dimensions*, *Phys. Rev.* **D 52** (1995) 4718 [hep-th/9407168] [INSPIRE].

JHEP02(2014)097

[34] G. Semenoff, I. Shovkovy and L. Wijewardhana, *Phase transition induced by a magnetic field*, *Mod. Phys. Lett.* **A 13** (1998) 1143 [hep-ph/9803371] [INSPIRE].

[35] G. Semenoff, I. Shovkovy and L. Wijewardhana, *Universality and the magnetic catalysis of chiral symmetry breaking*, *Phys. Rev.* **D 60** (1999) 105024 [hep-th/9905116] [INSPIRE].

[36] D. Khveshchenko, *Magnetic field-induced insulating behavior in highly oriented pyrolitic graphite*, *Phys. Rev. Lett.* **87** (2001) 206401 [cond-mat/0106261] [INSPIRE].

[37] V.G. Filev, C.V. Johnson and J.P. Shock, *Universal holographic chiral dynamics in an external magnetic field*, *JHEP* **08** (2009) 013 [arXiv:0903.5345] [INSPIRE].

[38] G.W. Semenoff and F. Zhou, *Magnetic catalysis and quantum Hall ferromagnetism in weakly coupled graphene*, *JHEP* **07** (2011) 037 [arXiv:1104.4714] [INSPIRE].

[39] S. Bolognesi and D. Tong, *Magnetic catalysis in AdS_4*, *Class. Quant. Grav.* **29** (2012) 194003 [arXiv:1110.5902] [INSPIRE].

[40] J. Erdmenger, V.G. Filev and D. Zoakos, *Magnetic catalysis with massive dynamical flavours*, *JHEP* **08** (2012) 004 [arXiv:1112.4807] [INSPIRE].

[41] S. Bolognesi, J.N. Laia, D. Tong and K. Wong, *A gapless hard wall: magnetic catalysis in bulk and boundary*, *JHEP* **07** (2012) 162 [arXiv:1204.6029] [INSPIRE].

[42] I.A. Shovkovy, *Magnetic catalysis: a review*, *Lect. Notes Phys.* **871** (2013) 13 [arXiv:1207.5081] [INSPIRE].

[43] M. Blake, S. Bolognesi, D. Tong and K. Wong, *Holographic dual of the lowest Landau level*, *JHEP* **12** (2012) 039 [arXiv:1208.5771] [INSPIRE].

[44] V.G. Filev and M. Ihl, *Flavoured large-N gauge theory on a compact space with an external magnetic field*, *JHEP* **01** (2013) 130 [arXiv:1211.1164] [INSPIRE].

[45] O. DeWolfe, D.Z. Freedman and H. Ooguri, *Holography and defect conformal field theories*, *Phys. Rev.* **D 66** (2002) 025009 [hep-th/0111135] [INSPIRE].

[46] J. Erdmenger, Z. Guralnik and I. Kirsch, *Four-dimensional superconformal theories with interacting boundaries or defects*, *Phys. Rev.* **D 66** (2002) 025020 [hep-th/0203020] [INSPIRE].

[47] D.A. Siegel et al., *Many-body interactions in quasi-freestanding graphene*, *P. Natl. Acad. Sci. USA* **108** (2011) 11365.

[48] N. Evans and E. Threlfall, *Chemical potential in the gravity dual of a $2+1$ dimensional system*, *Phys. Rev.* **D 79** (2009) 066008 [arXiv:0812.3273] [INSPIRE].

[49] V.G. Filev, *Hot defect superconformal field theory in an external magnetic field*, *JHEP* **11** (2009) 123 [arXiv:0910.0554] [INSPIRE].

[50] N. Evans, A. Gebauer, K.-Y. Kim and M. Magou, *Holographic description of the phase diagram of a chiral symmetry breaking gauge theory*, *JHEP* **03** (2010) 132 [arXiv:1002.1885] [INSPIRE].

[51] K. Jensen, A. Karch, D.T. Son and E.G. Thompson, *Holographic Berezinskii-Kosterlitz-Thouless transitions*, *Phys. Rev. Lett.* **105** (2010) 041601 [arXiv:1002.3159] [INSPIRE].

[52] N. Evans, A. Gebauer, K.-Y. Kim and M. Magou, *Phase diagram of the $D3/D5$ system in a magnetic field and a BKT transition*, *Phys. Lett.* **B 698** (2011) 91 [arXiv:1003.2694] [INSPIRE].

JHEP02(2014)097

[53] N. Evans, K. Jensen and K.-Y. Kim, *Non mean-field quantum critical points from holography*, *Phys. Rev.* **D 82** (2010) 105012 [arXiv:1008.1889] [INSPIRE].

[54] G. Grignani, N. Kim and G.W. Semenoff, *D3-D5 holography with flux*, *Phys. Lett.* **B 715** (2012) 225 [arXiv:1203.6162] [INSPIRE].

[55] V.G. Filev, M. Ihl and D. Zoakos, *A novel* $(2+1)$*-dimensional model of chiral symmetry breaking*, *JHEP* **12** (2013) 072 [arXiv:1310.1222] [INSPIRE].

[56] G. Grignani, N. Kim and G.W. Semenoff, *D7-$\bar{D}$7 bilayer: holographic dynamical symmetry breaking*, *Phys. Lett.* **B 722** (2013) 360 [arXiv:1208.0867] [INSPIRE].

[57] O. Bergman, N. Jokela, G. Lifschytz and M. Lippert, *Quantum Hall effect in a holographic model*, *JHEP* **10** (2010) 063 [arXiv:1003.4965] [INSPIRE].

[58] N. Jokela, G. Lifschytz and M. Lippert, *Magneto-roton excitation in a holographic quantum Hall fluid*, *JHEP* **02** (2011) 104 [arXiv:1012.1230] [INSPIRE].

[59] N. Jokela, M. Jarvinen and M. Lippert, *A holographic quantum Hall model at integer filling*, *JHEP* **05** (2011) 101 [arXiv:1101.3329] [INSPIRE].

[60] O. Bergman, N. Jokela, G. Lifschytz and M. Lippert, *Striped instability of a holographic Fermi-like liquid*, *JHEP* **10** (2011) 034 [arXiv:1106.3883] [INSPIRE].

[61] N. Jokela, M. Jarvinen and M. Lippert, *Fluctuations of a holographic quantum Hall fluid*, *JHEP* **01** (2012) 072 [arXiv:1107.3836] [INSPIRE].

[62] N. Jokela, G. Lifschytz and M. Lippert, *Magnetic effects in a holographic Fermi-like liquid*, *JHEP* **05** (2012) 105 [arXiv:1204.3914] [INSPIRE].

[63] J. Alicea and M.P.A. Fisher, *Interplay between lattice-scale physics and the quantum Hall effect in graphene*, *Solid State Commun.* **143** (2007) 504.

[64] C. Toke et al., *Fractional quantum Hall effect in graphene*, *Phys. Rev.* **B 74** (2006) 235417.

[65] K. Yang, S. Das Sarma and A.H. MacDonald, *Collective modes and skyrmion excitations in graphene* SU(4) *quantum Hall ferromagnets*, *Phys. Rev.* **B 74** (2006) 075423 [cond-mat/0605666] [INSPIRE].

[66] N. Peres, F. Guinea and A. Castro Neto, *Electronic properties of disordered two-dimensional carbon*, *Phys. Rev.* **B 73** (2006) 125411 [INSPIRE].

[67] D.V. Khveshchenko, *Composite Dirac fermions in graphene*, *Phys. Rev.* **B 75** (2007) 153405.

[68] N. Shibata and K. Nomura, *Coupled charge and valley excitations in graphene quantum Hall ferromagnet*, *Phys. Rev.* **B 77** (2008) 235426 [arXiv:0803.2418] [INSPIRE].

[69] M.O. Goerbig and N. Regnault, *Analysis of a* SU(4) *generalization of Halperin's wave function as an approach towards a* SU(4) *fractional quantum Hall effect in graphene sheets*, *Phys. Rev.* **B 75** (2007) 241405 [cond-mat/0701661] [INSPIRE].

[70] K.I. Bolotin, F. Ghahari, Mi.D. Shulman, H. L. Stormer and P. Kim, *Observation of the fractional quantum Hall effect in graphene*, *Nature* **462** (2009) 196.

[71] X. Du et al., *Fractional quantum Hall effect and insulating phase of Dirac electrons in graphene*, *Nature* **462** (2009) 192.

[72] A.F. Morpurgo, *Condensed-matter physics: Dirac electrons broken to pieces*, *Nature* **462** (2009) 170.

JHEP02(2014)097

[73] E. Witten, SL(2, $\mathbb{Z}$) *action on three-dimensional conformal field theories with Abelian symmetry*, in *From fields to strings, volume 2*, M. Shifman, World Scientific, Singapore (2009), hep-th/0307041 [INSPIRE].

[74] C. Burgess and B.P. Dolan, *Particle vortex duality and the modular group: applications to the quantum Hall effect and other* 2*D systems*, *Phys. Rev.* **B 63** (2001) 155309 [hep-th/0010246] [INSPIRE].

[75] C. Burgess and B.P. Dolan, *The quantum Hall effect in graphene: emergent modular symmetry and the semi-circle law*, *Phys. Rev.* **B 76** (2007) 113406 [cond-mat/0612269] [INSPIRE].

[76] J.H. Brodie, L. Susskind and N. Toumbas, *How Bob Laughlin tamed the giant graviton from Taub-NUT space*, *JHEP* **02** (2001) 003 [hep-th/0010105] [INSPIRE].

[77] S. Hellerman and L. Susskind, *Realizing the quantum Hall system in string theory*, hep-th/0107200 [INSPIRE].

[78] M. Fujita, W. Li, S. Ryu and T. Takayanagi, *Fractional quantum Hall effect via holography: Chern-Simons, edge states and hierarchy*, *JHEP* **06** (2009) 066 [arXiv:0901.0924] [INSPIRE].

[79] R.G. Leigh, A.C. Petkou and P.M. Petropoulos, *Holographic fluids with vorticity and analogue gravity*, *JHEP* **11** (2012) 121 [arXiv:1205.6140] [INSPIRE].

[80] N. Jokela, G. Lifschytz and M. Lippert, *Holographic anyonic superfluidity*, *JHEP* **10** (2013) 014 [arXiv:1307.6336] [INSPIRE].

JHEP02(2014)097